

Article

Unveiling Iso- and Aniso-Hydric Disparities in Grapevine—A Reanalysis by Transcriptome Portrayal Machine Learning

Tomas Konecny ^{1,2,*}, Armine Asatryan ^{1,3,†}, Maria Nikoghosyan ^{1,4} and Hans Binder ^{1,2}¹ Armenian Bioinformatics Institute, Yerevan 0014, Armenia; armine.asatryan@abi.am (A.A.); maria.nikoghosyan@abi.am (M.N.); binder@izbi.uni-leipzig.de (H.B.)² Interdisciplinary Centre for Bioinformatics, University of Leipzig, 04107 Leipzig, Germany³ Group of Plant Genomics, Institute of Molecular Biology, National Academy of Sciences of Armenia, Yerevan 0014, Armenia⁴ Bioinformatics Group, Institute of Molecular Biology, National Academy of Sciences of Armenia, Yerevan 0014, Armenia

* Correspondence: tomas.konecny@abi.am

† These authors contributed equally to this work.

Abstract: Mechanisms underlying grapevine responses to water(-deficient) stress (WS) are crucial for viticulture amid escalating climate change challenges. Reanalysis of previous transcriptome data uncovered disparities among isohydric and anisohydric grapevine cultivars in managing water scarcity. By using a self-organizing map (SOM) transcriptome portrayal, we elucidate specific gene expression trajectories, shedding light on the dynamic interplay of transcriptional programs as stress duration progresses. Functional annotation reveals key pathways involved in drought response, pinpointing potential targets for enhancing drought resilience in grapevine cultivation. Our results indicate distinct gene expression responses, with the isohydric cultivar favoring plant growth and possibly stilbenoid synthesis, while the anisohydric cultivar engages more in stress response and water management mechanisms. Notably, prolonged WS leads to converging stress responses in both cultivars, particularly through the activation of chaperones for stress mitigation. These findings underscore the importance of understanding cultivar-specific WS responses to develop sustainable viticultural strategies in the face of changing climate.

Keywords: grapevine; climate changes; water(-deficient) stress; transcriptome portrayal; SOM machine learning; stilbenoid biosynthesis; thiamine biosynthesis



Citation: Konecny, T.; Asatryan, A.; Nikoghosyan, M.; Binder, H. Unveiling Iso- and Aniso-Hydric Disparities in Grapevine—A Reanalysis by Transcriptome Portrayal Machine Learning. *Plants* **2024**, *13*, 2501. <https://doi.org/10.3390/plants13172501>

Academic Editors: Giovan Battista Mattii and Eleonora Cataldo

Received: 27 July 2024

Revised: 2 September 2024

Accepted: 4 September 2024

Published: 6 September 2024



Copyright: © 2024 by the authors. Licensee MDPI, Basel, Switzerland. This article is an open access article distributed under the terms and conditions of the Creative Commons Attribution (CC BY) license (<https://creativecommons.org/licenses/by/4.0/>).

1. Introduction

Vitis vinifera, being a cornerstone in the global wine industry, faces unprecedented challenges in the era of climate change. Among these challenges, drought stands out as one of the pivotal factors causing water(-deficient) stress (WS), influencing grape ripening and overall fruit quality. As global temperatures rise and precipitation patterns become increasingly unpredictable, the study of WS in *Vitis vinifera* has become paramount for ensuring the resilience of vineyards and the sustainability of wine production.

Current climate change scenarios have brought about shifts in weather patterns, leading to prolonged periods of water scarcity and extreme climatic events. These changes pose a significant threat to viticulture, impacting grapevine physiology, grape quality, and wine production. WS, characterized by a deficiency in water availability relative to the plant's demand, triggers a cascade of physiological responses in *Vitis vinifera*, affecting its growth, photosynthesis, and metabolic processes [1–4]. Notably, grapevines have evolved two distinct mechanisms, isohydric and anisohydric, to navigate the complex interplay between water availability and demand [5–9]. Isohydric cultivars regulate water potential by actively adjusting stomatal conductance, conserving water during limited availability,

and prioritizing water status regulation over continuous carbon assimilation. Conversely, anisohydric cultivars maintain sustained carbon assimilation even under declining water availability, with a more permissive control over stomatal conductance [10–12]. While promoting growth and productivity, this strategy exposes grapevines to higher risks of hydraulic failure under severe water deficit situations [9,13,14].

The investigation of these isohydric and anisohydric mechanisms gains significance in deciphering the adaptive strategies of *Vitis vinifera* to varying water conditions [15–17]. The importance of such research is heightened by the need to develop resilient grape cultivars or drought-resistant rootstocks and implement sustainable viticultural practices in response to the changing climate.

Even though both isohydric and anisohydric mechanisms in different grapevine cultivars are well-known and studied at the transcriptomics level [15], current advancements in the field of artificial intelligence (AI) and machine learning (ML) and their applications in analyzing molecular biology data offer exciting possibilities. AI- and ML-powered analyses, particularly through techniques like self-organizing maps (SOM), have the potential to unlock a deeper understanding of the underlying mechanisms and biological pathways that occur at specific time points during stress treatments relevant to viticulture [18]. SOM is a type of artificial neural network that can visualize high-dimensional data like gene expression profiles. By analyzing transcriptomic data using SOM, hidden patterns and relationships between genes can be identified and visualized, enhancing understanding of the underlying mechanisms governing grapevine responses to abiotic stress conditions caused, for instance, by cold temperatures or by water limitation.

A previous study [15] delved into how grapevine transcriptomes respond to WS at the molecular level. The studied isohydric cultivar ('Montepulciano') exhibited a faster transcriptome response after WS imposition, with rapid modulation of genes related to abscisic acid (ABA), a stress response hormone, and quicker expression of heat-shock protein (HSP) genes. On the other hand, an anisohydric cultivar ('Sangiovese') displayed early and robust induction of reactive oxygen species (ROS)-scavenging enzymes, molecular chaperones, and abiotic-stress-related genes in response to deficiency of water. While this research provides valuable insights, it is important to recognize that the genes identified by significance analysis of microarrays (SAM) represent a portion of the grapevine's response to WS [19]. Here, we apply SOM omics portrayal to these data to analyze the transcriptomic response of isohydric or anisohydric grapevines under water deficit conditions. SOM transcriptomics portrayal was developed to extract and interpret complex patterns from multidimensional transcriptomic data [20], and it has been applied recently to cold stress acting on *Vitis vinifera* and, particularly, to describe the transcriptomics trajectories of the grapevine plant under changing environmental conditions [18]. Our aim is to compare trajectories associated with drought response in the isohydric and anisohydric grapevine categories. We show that isohydric MP initially maintains a muted transcriptional response, prioritizing transcripts for normal growth (phloem development) before potentially shifting towards activation of stress response processes for survival. Conversely, anisohydric SG displays a rapid transcriptional response, initially focusing on stress alleviation (ketoreductase, arogenate) and water management (lignin catabolism, chitinase activity) before upregulating thiamin biosynthesis, a pathway potentially linked to broader abiotic stress tolerance. Despite their distinct genetic backgrounds related to water-use efficiency, both cultivars eventually converge toward shared responses under prolonged drought conditions.

2. Results

2.1. WS Influences Gene Expression Trajectories in Distinct Cultivars

"Drought" stresses the plants due to a hydric deficiency, i.e., the effect of water reserve (e.g., soil water deficit) defined as the difference between the maximum and the actual water availability (field capacity). The experimental setup of Dal Santo and colleagues modeled such (deficient) WS conditions to study physiological responses based on transcriptomic data [15]. They achieved it by comparing one isohydric and one anisohydric cultivar under

well-watered and water-stressed conditions as a time series of three measurements in three biological replicates. Our SOM method provides “portrait” images of each of those 36 measurements, visualizing their individual transcriptome landscapes in terms of red overexpression and blue underexpression “spots” (Figure 1A). Note that SOM portrayal methods provide individual images of each sample, which visualize the expression landscape of nearly 30,000 single genes using a color code from blue (low expression) to dark red (high expression) for “spot”-like clusters of co-regulated genes. All images apply the same coordinate system of gene distribution, meaning that they can be directly compared and used for downstream analyses such as similarity and trajectory analysis as well as function mining by means of gene set enrichment analysis (see [20] for a detailed description of the method). Our focus remains on studying changing expression patterns under progressing WS. For an overview, we generated a pairwise correlation heatmap between all portraits. It revealed that the data separated between the two cultivars in terms of two distinct clusters of samples with similar expression patterns evident as dark-red squares reflecting positive correlations between them (Figure 1B). The small red quadrants along the diagonal refer to the similarities of the replicates, as expected. Interestingly, off-diagonal correlations were also observed referring to similarities between STRS and CTRL conditions at T1 and T2, between the two cultivars at T3, as well as to dissimilarities between time points T1 and T3 under WS conditions (see red and blue areas in Figure 1B, respectively). Independent component analysis (ICA) transforms the correlation matrix into a spatial distribution of the samples in the coordinate system of the first three independent components (IC1–IC3). Interestingly, it indicates linear trajectories for each of the cultivars (MP versus SG separated along component IC1) progressing with time (T1 to T3), mostly along IC2 and showing an extra increment under WS (Figure 1C). The so-called “Sample SOM” (Figure 1D) projects these relations into two dimensions. It also shows the two parallel temporal trajectories slightly converging at T3, suggesting an offset between the WS transcriptomic mechanisms of both cultivars and similar stress response mechanisms over time acting in MP and SG.

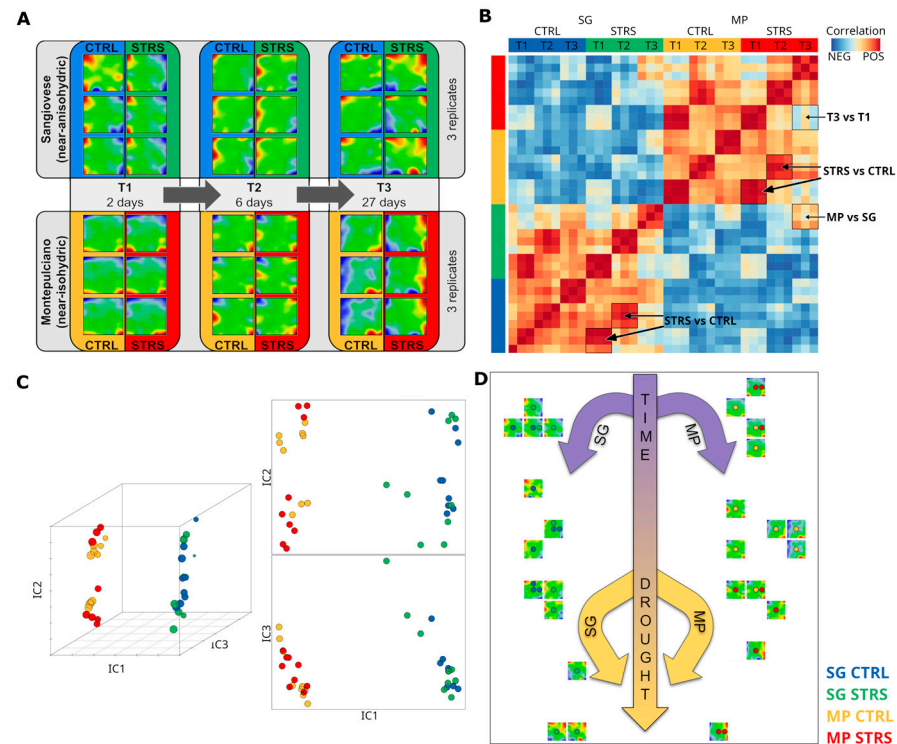


Figure 1. Transcriptome portrayal of the WS experiment reveals distinct trajectories for isohydric (MP) and anisohydric (SG) cultivars. (A) SOM transcriptome portraits of all samples studied. (B) The pairwise correlation map of the SOM portraits indicates two distinct clusters for the two cultivars, correlation squares along the diagonal due to the replicates, and off-diagonal correlations between different time

points and stress-induced effects in both cultivars (see arrows). (C) The independent component plot of the portraits shows linear trajectories along the IC2 axis of both cultivars. IC1, IC2, and IC3 denote the first three independent components. (D) Sample SOM represents a two-dimensional presentation of the trajectories: Transcriptome trajectories separate due to isohydric and anisohydric cultivars in the horizontal direction and develop with time vertically with an additional increment due to WS. Dots inside each “Sample SOM” represent samples. The color code of samples is indicated in the bottom right corner.

In summary, SOM portrayal visualizes the expression data of grapevine genes as sample-specific, “individual” images, which enables their visual inspection and comparison. This analysis reveals two different transcriptome clusters for the selected isohydric and anisohydric cultivars, giving rise to two virtually parallel trajectories in sample space, which are indicative of a basic difference of their transcriptomes but similar time courses of their transcriptomes under WS conditions.

2.2. Different Water Management Strategies Regulate Similar Genes under Lasting WS

To better understand the changing gene expression patterns behind the observed trajectories, we analyzed the SOM portraits in more detail. The SOM algorithm clusters genes with correlated expression profiles across the time courses together into red “spot-like” modules in the portraits, which were summarized into one overview “Overexpression map” (Figure 2A, part above; for a detailed description of the SOM portrayal method see the Materials and Methods section and references cited therein). Overall, we identified six such modules labeled with capital letters A–F. They collect the most variant genes, and contain around 300 to 600 genes each (Figure 2A,B; lists of genes in the spots are given in Table A1). The expression profiles of the spots divide into characteristic time courses of both cultivars, namely: genes upregulated permanently in SG and downregulated in MP (spot A); the antagonistic profile (spot B); genes activated in both cultivars at T1 (spot C), T2 (spot D), or T3, however differently expressed between SG and MP (spot E); and, finally, genes upregulated at T3 in both cultivars (spot F, see Figure 2B).

Gene set overrepresentation analysis of the gene lists of each of the spots provides a first glimpse at their functional background (Figure 2B). For example, the genes in spot A, differentially upregulated in SG compared with MP, are related to steroid and lipid biosynthesis, while genes in spot B, differentially upregulated in MP compared with SG, are related to stilbenoid, diarylheptanoid, and gingerol biosynthesis. These different functions of the transcriptional programs thus indicate the basic differences between both cultivars at the gene expression level. Temporal progression is driven in both cultivars by the activation of genes related to cell wall pathogen-defensive functions (T1, spot C); different transcription factors such as MYB, WRKY, and AS2 (T2, spot D); sugar biosynthesis (T3, spot E); and chaperones under long-lasting WS (T3, spot F). These factors act as master regulators, turning on genes involved in various drought tolerance mechanisms [21]. MYB transcription factors are known to regulate genes for osmoprotectant synthesis, secondary metabolite production, and WS responses [22–27]. WRKY factors are involved in signaling pathways, hormonal routes, defense responses, antioxidant production, and regulation of other stress-responsive genes [28]. AS2 (ASYMMETRIC LEAVES2) plays a co-opted role in stomatal regulation and water use efficiency, with a key role in flat symmetric leaf formation [29].

To better identify subtle changes in expression patterns in the SOM portraits, we generated mean waterline portraits averaged over all time points referring to CTRL and STRS conditions of MP and SG, respectively (Figure 2C, part above). They highlight regions of up- and downregulated genes in red and blue, respectively, and thus enable us to visualize subtle modulations of gene expression levels more clearly than the standard portraits shown in Figure 1. Two different trajectories for SG and MP in gene space under WS can be identified, pointing in clock- and counterclockwise directions, respectively, and both converging in the right upper corner around spot F (see arrows).

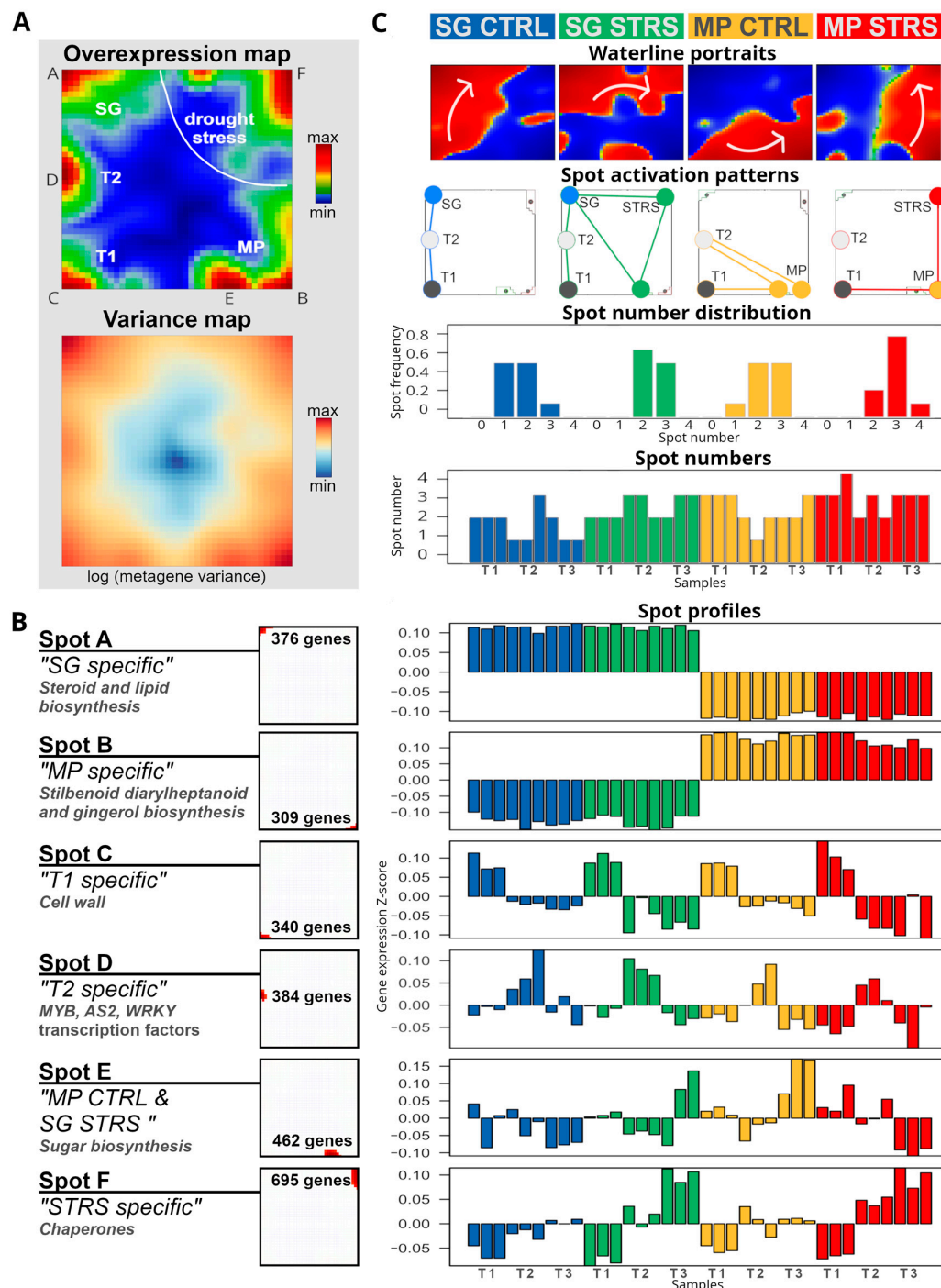


Figure 2. Transcriptome dynamics under WS in isohydric (MP) and anisohydric (SG) water management. (A) The regions of characteristic overexpression as red areas labeled A–F (see “Overexpression map”) agree with regions of highest expression variance (see “Variance map”). (B) Spots usually contain a few hundred genes of different functional contexts (left). Expression profiles of the spots across all conditions reveal characteristic courses of transcriptomic co-regulation (right). (C) Transcriptome dynamics under WS is characterized by waterline portraits revealing different stress trajectories for SG and MP (gray arrows), time, as well as by spot activation patterns (spots jointly activated in the portraits are connected by lines at the time points indicated). The number of jointly expressed spots increases under WS, thus indicating a more complex transcriptomic pattern compared to the controls (see text).

The spots identified in Figure 2A are activated in various combinations, depending on the experimental conditions. This results in diverse configurations of the gene expression landscapes, as depicted by the networks of spot activation (Figure 2C, second row from the top, co-expressed spots are linked by lines). Note that the activation pattern follows the arrows in the waterline portraits. For SG, the spot modules progressively activate along the left and upper edges of the map. For MP, the spot modules activate along the lower and right edges. The activation patterns of SG and MP converge in spot F under lasting WS at T3. The number of jointly activated spots is slightly larger in SG compared to MP and increases under stress, thus reflecting a more complex transcriptional pattern (Figure 2C, the two rows from the bottom). This increased number of jointly activated spots reflects a higher complexity of the underlying transcriptional programs, which slightly increases under lasting WS.

Hence, SOM portrayal complements the two different trajectories for the isohydric and anisohydric cultivars observed in the sample space (see previous subsection) by trajectories in the gene expression space, which enables identification of jointly and differently activated transcriptional programs as a function of the cultivars, the WS conditions, and the time points.

2.3. Topology of Transcriptional Programs under Progressing WS

As shown in the previous section, our spot activation analysis revealed two different trajectories in the gene expression landscape pointing from T1 to T3 in the clockwise and counterclockwise direction for the SG and MP cultivars, respectively (Figure 3A). We asked about the transcriptional programs associated with the different sets of genes taken from the spots to better understand the functional background of the observed WS dynamics. Spot A and B include genes antagonistically activated in SG and MP, respectively, forming a sort of background expression for the anisohydric and isohydric cultivars, respectively. The progression from T1 to T3 along IC2 in ICA analysis (see Figure 1C above) is driven by the sequential activation of spots C, D, and F, respectively (see the scheme in Figure 3B). Hence, the topology of gene activations as visualized by the SG- and MP-trajectories in the three-dimensional gene expression landscape (Figure 3A) and, alternatively, by the spot activation workflow in Figure 3B rationalizes the common and different properties of the isohydric and anisohydric cultivar dynamics under WS.

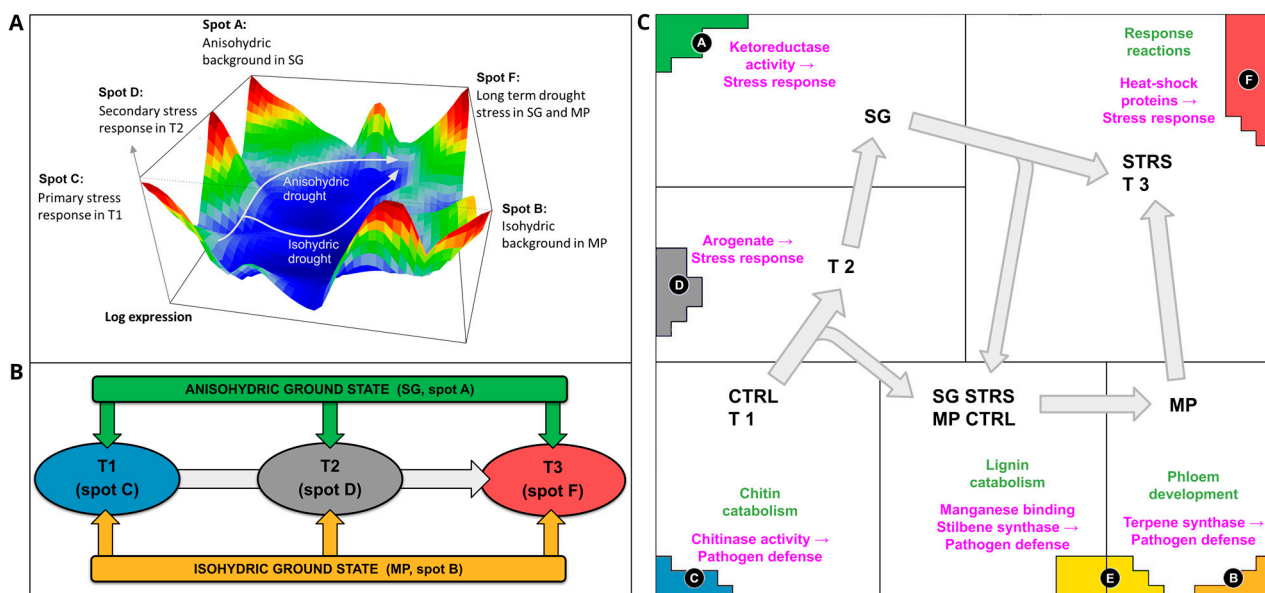


Figure 3. Topology of expression trajectories under WS. (A) The stress trajectories in the three-dimensional expression landscape. (B) Schematic spot activation along the T1-T2-T3 trajectory. (C) Gene ontology enrichment in spots A–F (biological processes in green, molecular functions in pink text).

Figure 3C provides a functional map associating the genes in the spots with the underlying biological functions using gene set enrichment analysis. The anisohydric SG, exhibiting open stomata and being more prone to water deficiency stress, remains consistently predisposed to WS. The genes specifically activated in SG accumulate in spot A (Figure 3C). They associate with functions such as steroid and lipid biosynthesis. We found an enrichment of ketoreductase activity (GO:0045703). Hence, the upregulation of ketoreductases observed in SG background (spot A) can serve as an initial indication of stress accompanied by the plant response to reactive oxygen species [30,31].

In contrast to SG, the isohydric cultivar MP is better adapted to sustain water levels during drought, which is demonstrated by the upregulation of genes associated with plant normal growth, development, transportation, and signaling pathways (see spots B and E in Figure 3C). For instance, some of these genes are linked to stilbenoid, diarylheptanoid, and gingerol biosynthesis. Additionally, there is also GO enrichment in phloem development (GO:0010088), promoting the development of phloem cells, and terpene synthase activity (GO:0010333) that plays a role in plant defense response to environment and pathogens [32].

At the first time point T1, genes in spot C (Figure 3C) upregulate in both MP and SG cultivars. They are enriched by gene sets involved in chitin catabolism (GO:0006032) and cell wall development. A strengthened cell wall (chitin and lignin) is a common defense strategy against drought [33,34], as well as pathogens [35]. The second time point, T2, upregulated genes in spot D (Figure 3C), which is occupied by genes coding transcription factors (MYB, AS2, WRKY). The transcriptional reprogramming mediated by MYB, AS2, and WRKY transcription factors orchestrates broader regulatory networks involved in stress signaling, defense responses, and developmental adjustments reacting to prolonged water shortage. The MYB transcription factors, for example, regulate the secondary metabolism, hormone signaling, and stress responses, contributing to drought tolerance mechanisms [27,36,37]. AS2 transcription factors participate in leaf morphology and physiology which optimizes the efficiency of water management under drought conditions [29,38]. WRKY transcription factors, the integral components of many vines' stress signaling pathways, coordinate biological processes associated with stress tolerance, such as scavenging of ROS, osmotic regulation, and ABA signaling [39]. There is also an enrichment in GO molecular activity of arogenate dehydrogenase NADP+ (GO:0033730) in spot D. Arogenate is a precursor of phenylalanine that plays a significant role in plant abiotic stress responses [40–42]. Hence, with the increasing time under drought, more comprehensive genes are involved in the WS response.

Spot E is upregulated at T3 in SG (under STRS) and MP (under CTRL), thus inducing a certain asymmetry between both trajectories. The gene list of this spot is enriched by sugar biosynthesis genes. For anisohydric cultivars such as SG, sugar serves as an osmoprotectant that maintains cellular hydration under lasting WS [43]. Additionally, this spot is enriched by genes related to lignin catabolism (GO:0046274), playing a role in water management, manganese ion binding (GO:0030145), and trihydroxystilbene synthesis (GO:0050350), considered to be important for pathogen defense [44–46]. Hence, osmoprotection and pathogen response become activated in the anisohydric cultivar under lasting WS, while the isohydric cultivar activates these functions under water excess.

STRS-specific spot F (Figure 3C) contains genes enriched by heat-shock/protein-complex oligomerization proteins (GO:0051259) from the family HSP20 acting as molecular chaperones. Such chaperones help plants fight against WS by facilitating protein folding, assembly, stabilization, and degradation [47]. Despite the differences in transcriptomes between SG and MP in T1/T2, water deficiency induces a similar response in prolonged exposure (T3).

Taken together, different “ground state” functions related to lipid and steroid biosynthesis in SG and plant growth functions in isohydric MP give rise to their specific trajectories, which both progress under WS sequentially by activation of transcription factors such as MYB, AS2, and WRKY, ABA-signaling, and arorgenate-mediated stress response, and after lasting WS finally express HSP coding genes. An asymmetry in WS dynamics between SG

and MP is related to osmoprotection by sugar biosynthesis and lignin catabolism in SG STRS and in MP under CTRL conditions, respectively.

2.4. Isohydric Strategy Is Characterized by Biosynthesis of Stilbenoid and Its Derivatives

Our analysis of gene expression patterns revealed that the isohydric grape cultivar, known for its water-conserving strategies, appears to activate stilbenoid biosynthesis as a marker of drought tolerance, partly in its ground state. Genes related to stilbenoid biosynthesis distribute in a characteristic fashion in the expression landscape with a certain asymmetry towards the MP trajectory (Figure 4A). Although located mostly outside the spots due to the smaller variance in their expression, they can be assigned to different conditions, as discussed in the previous subsection. The heatmap in Figure 4B explicitly provides their expression profiles, revealing their time-dependent activation under the different conditions, which shows their biased upregulation in the isohydric MP cultivar.

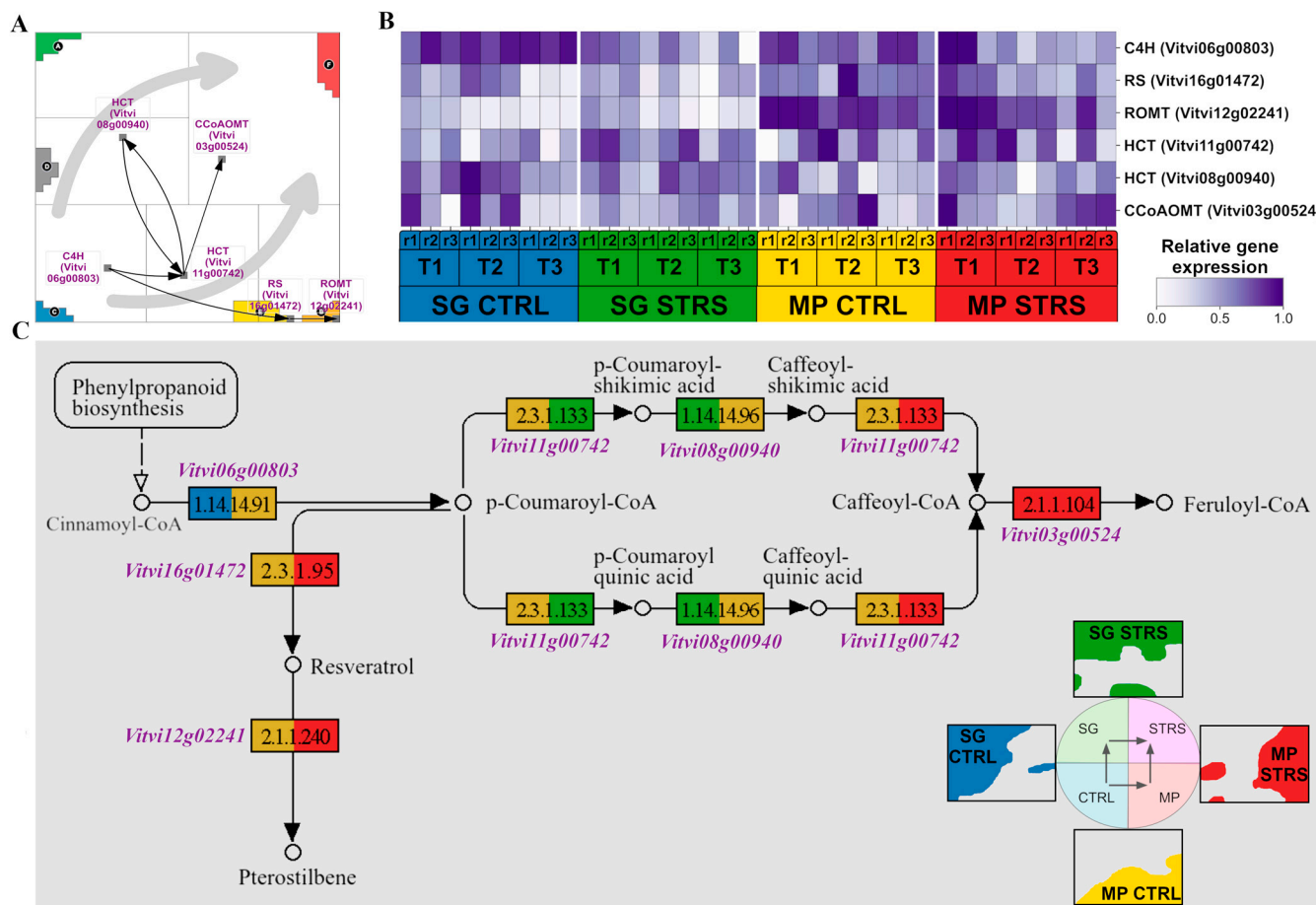


Figure 4. Stilbenoid, diarylheptanoid, and gingerol biosynthetic pathway. (A) Genes of the pathway (downstream flow visualized by black arrows) are along the two STRS trajectories (gray arrows), indicating their condition-specific activation. (B) The heatmap shows the expression changes in response to WS. (C) KEGG pathway with gene color code derived from their positions in the SOM portrait indicated by the colored waterline portraits of SG CTRL and STRS and MP CTRL and STRS (see the lower right part).

For a closer look, we mapped these activation patterns on the stilbenoid KEGG pathway topology, where the gene boxes are colored according to the condition-dependent activation (Figure 4C). CINNAMATE 4-HYDROXYLASE (C4H), encoded by the gene *Vitvi06g00803*, is an important precursor enzyme for stilbenoid biosynthesis. The gene was found to be upregulated in both SG and MP under optimal CTRL water supply conditions, as indicated by the blue and dark yellow colors, respectively. C4H catalyzes the

hydroxylation of trans-cinnamic acid to produce p-coumaric acid, an important intermediate in the biosynthesis of various compounds, including stilbenoids [48]. Next, there is an enzyme HYDROXYCINNAMOYL-CoA:SHIKIMATE/QUINATE TRANSFERASE (HCT-HST/HQT), whose instability allows for various reactions to occur [49,50]. This enzyme is encoded by the genes *Vitvi11g00742* and *Vitvi08g00940*, which exhibited interesting expression dynamics. *Vitvi11g00742* showed higher expression in MP CTRL during the initial reaction, whereas it was upregulated in SG STRS. This enzyme mediates the formation of p-Coumaroyl shikimic acid and p-Coumaroyl quinic acid [50,51]. Subsequent reactions showed differential expression patterns, with *Vitvi11g00742* shifting its overexpression entirely to MP STRS. The enzyme Caffeoyl-CoA O-METHYLTRANSFERASE (CCoAOMT), encoded by gene *Vitvi03g00524*, emerged as a dominant player in (isohydric) MP STRS as well. It is known to respond to water deficiency stress [52]. Other downstream enzymes involved in the synthesis of stilbenoids, namely RESVERATROL SYNTHASE (RS) and RESVERATROL O-METHYLTRANSFERASE (ROMT), were found to be exclusively overexpressed in MP STRS conditions. The RS enzyme, encoded by *Vitvi16g01472*, catalyzes the condensation of malonyl-CoA with p-Coumaroyl-CoA to form resveratrol [53], while the enzyme ROMT (encoded by *Vitvi12g02241*) methylates the resveratrol to produce a pterostilbene [54]. All these genes exhibited higher expression levels in MP under both control and stress conditions, suggesting a potential role for resveratrol and pterostilbene in response to water deficiency stress in MP in agreement with the topology of WS transcriptome dynamics (see Figure 3C).

In summary, the detailed mapping of gene expression patterns onto the stilbenoid pathway elucidated the overall asymmetric role of various members of this pathway in MP's and SG's distinct responses to WS, where, notably, resveratrol biosynthetic genes were uniquely upregulated in the isohydric MP.

2.5. Biosynthesis of Thiamine Is Promoted under WS Conditions

Next, we aimed to elucidate the thiamine biosynthesis pathway in grapevines (Figure 5). This pathway was shown to react under conditions of low-temperature stress in *Vitis vinifera* [18] and was assumed to play an important role also under WS conditions [55]. The “gene map” of the thiamine biosynthesis pathway genes, as well as their expression heatmap, reveal the gene activation across the whole SOM landscape except the T1-specific area (Figure 5A,B). As for the pathway of biosynthesis of stilbenoid and its derivatives, we transferred the gene expression profiles into the KEGG pathway topology (Figure 5C). Under control conditions, both MP and SG cultivars exhibited nearly stable expression of genes involved in thiamine biosynthesis. These genes encode enzyme isoforms, including THIAZOLE (TH1), PYRIMIDINE SYNTHETASE (THIC), and THIAMINE PYROPHOSPHOKINASE (TPK/THIN), which plays a role in synthesizing the active form of thiamine. In plants, three forms of thiamine are physiologically active: free thiamine, thiamine monophosphate, and thiamine pyrophosphate. The Enzyme Commission number is depicted by the colored (blue, yellow) rectangles in the pathway diagram (see Figure 5C). Notably, the expression of these genes in both cultivars is similar also under WS, indicating a basal level of thiamine biosynthesis activity in grapevine plants.

Under WS, both cultivars exhibited the upregulation of structural genes, encoding isoforms of the enzyme 1-DEOXY-D-XYLULOSE-5-PHOSPHATE SYNTHASE (DXS). DXS is associated with the precursor production for both thiamine and isoprenoid biosynthesis [56], particularly DXP production from glycolysis. Isoprenoids, which have a positive correlation with the level of DXP transcript [57], play crucial roles in plant stress tolerance mechanisms [58]. Other studies have shown that the overexpression of DXS leads to increased chlorophyll and carotenoid content [59]. Furthermore, under the stress conditions, a cluster of genes was upregulated at the final stage of the pathway. Products of these genes convert the active form of thiamine, thiamine diphosphate (TPP), either to thiamine triphosphate (*Vitvi01g001564*, *Vitvi17g00142*, *Vitvi11g00609*, *Vitvi17g00137*, *Vitvi14g01574*, *Vitvi13g00202*) or thiamine monophosphate (*Vitvi04g01575*).

The grapevine gene *Vitvi11g01303*, encoding a probable enzyme 1-DEOXY-D-XYLULOSE-5-PHOSPHATE SYNTHASE2 (DXS2), exhibits upregulation in SG STRS compared to SG CTRL and even higher overexpression in MP STRS (Figure 5B). The presence of multiple DXS isoforms with distinct expression patterns in both cultivars suggests a potentially intricate regulatory mechanism governing DXP production in response to WS. The third precursor gene in thiamine biosynthesis, *Vitvi07g01408*, producing an enzyme L-CYSTEINE DESULFURASE 1 (LCD), provides the essential sulfur atom for thiazole precursor synthesis [60]. It was notably overexpressed under the WS compared to control conditions.

In summary, our analysis shows the various activations of thiamine biosynthesis genes under WS, from the initiation of precursor production to the final conversion of thiamine di-/tri- phosphate. This comprehensive understanding offers valuable insights into the distinct responses of MP and SG cultivars, potentially influencing their resilience to prolonged water deficit.

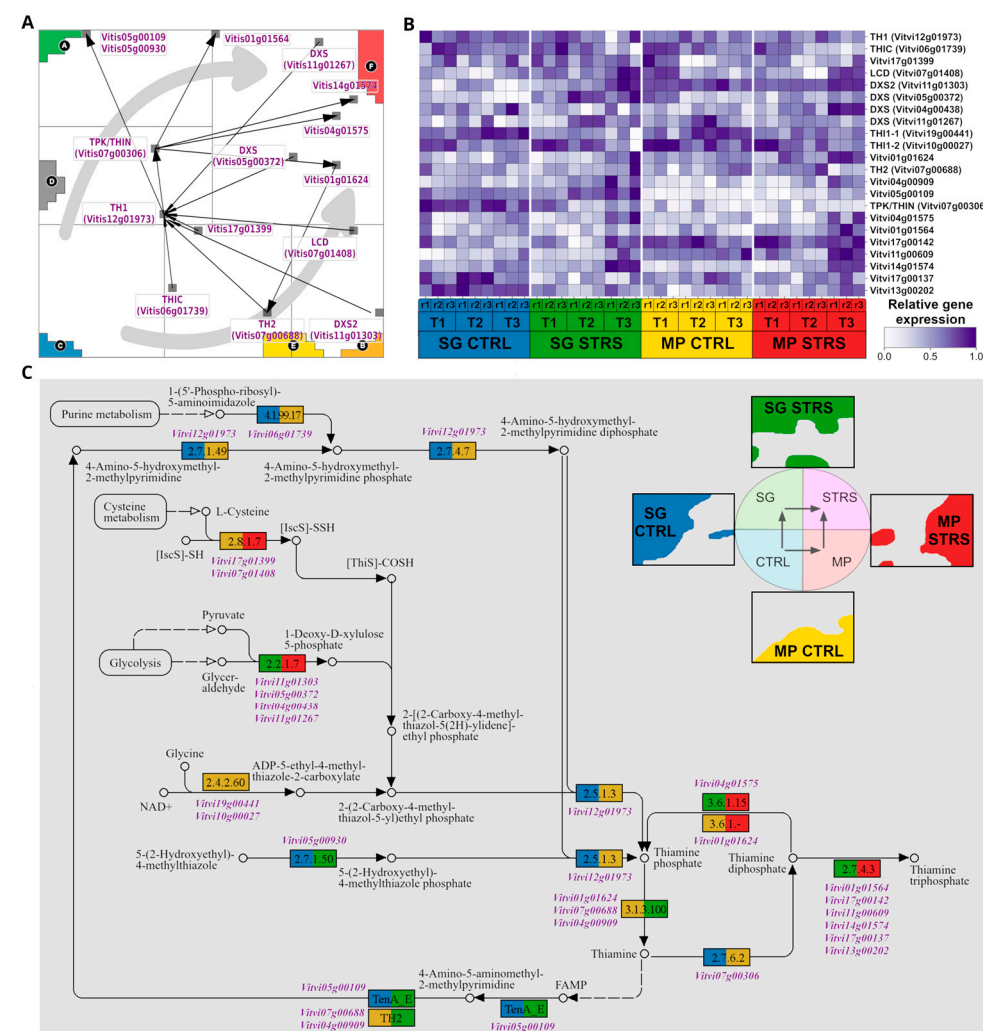


Figure 5. Thiamine biosynthetic pathway. (A) Map of the pathway (downstream flow visualized by black arrows). Genes accumulate in areas related to stress response, and the two STRS trajectories are shown by gray arrows. (B) Heatmap depicting the thiamine biosynthetic pathway gene expression in response to WS. (C) KEGG pathway with gene color code derived from their positions in the SOM portrait indicated by the colored waterline portraits of SG CTRL and STRS and MP CTRL and STRS (see the upper right part).

2.6. Exploring Differentially Expressed Genes Taken from the Original Study

Mapping of specifically modulated genes from the previous study [15] into our SOM landscape supports our results regarding a set of about 6000 highly differentially expressed genes (Figure A1). SOM portrayal, however, disentangles and visualizes in detail their covariance structure not evident from the original list. Notably, SOM portrayal distributes these genes across a transcriptome landscape, obeying the topology of transcriptomic co-regulation networks. Specifically, modulated genes in SG and MP fit into the WS trajectories extracted from the SOM analysis and visualized by the upregulated regions of the waterline portraits, as expected (Figure A2). However, SOM analysis more clearly disentangles the modulated genes into distinct modules of coregulation with distinct functional impact and, moreover, extracts higher genes of stronger variance compared with the significance analysis of microarrays (SAM) and ANOVA algorithms applied in the original paper [15] and the references cited therein. SAM should be used with caution because of the limitations of the method, particularly in overrating threshold settings and variance corrections [61].

Up- and downregulated genes, due to the WS, extract additional modules of co-regulated genes with different functional impacts, such as photosynthesis and DNA repair (Figure A3). Finally, we also considered genes differentially expressed under a “recovery from the WS” (i.e., re-watering 70 days after the onset of the WS), which indicates the partial reversal of the gene expression changes caused by prolonged WS (Figure A4).

Our SOM analysis demonstrates highly similar differential gene expression patterns for the genes previously reported. SOM considers genes of higher variance, which extends the range of the functional impact of WS dynamics. Note also that our SOM landscape reflects expression patterns without pre-selecting case vs. control conditions (e.g., STRS vs. CTRL, SG vs. MP), which were addressed in downstream analyses as applied above. It thus provides a sort of holistic modular transcriptomic map that considers the cultivar, conditions, and time points independently, which is required for estimating the trajectories of WS in the SOM landscape and not explicitly available using the SAM and ANOVA approaches.

3. Discussion

In this study, we reanalyzed whole-genome transcriptional microarray data of *Vitis vinifera* leaves [15] by applying the SOM clustering algorithm [62,63], which has previously been successfully employed in analyzing gene expression data on grapevine cultivars under low-temperature stress conditions [18]. We are motivated for this study by a series of key advantages of SOM machine learning, such as high-resolution clustering into function-relevant modules of co-regulated genes, intuitive visualization of whole transcriptome landscapes with single-sample resolution (SOM portrayal), the combination of dimension and redundancy reduction with whole data processing, statistical power of feature selection and tracking expression trajectories in a topology-aware transcriptome landscape, which, overall, enabled the detailed analysis of gene expression changes over the stress period (2, 6, and 27 days), to compare both isohydric and anisohydric strategies of two selected cultivars against WS. For a detailed description of the method and its strength in different applications, we refer to our previous work [20,64–66]. Here we continue our studies on aspects of genomic regulation of grapevine physiology suffering from abiotic stress after considering cold temperature stress [18].

The isohydric and anisohydric cultivars show distinct physiological and morphological changes under WS [5,6,15,67–69]. To understand the underlying gene regulation of drought-responsive processes at the transcriptome and pathway levels in two grapevine genotypes differing in water management strategy, we performed SOM portrayal and WS trajectory analysis in sample and gene space in combination with detailed knowledge mining of the patterns of the identified coregulated genes. The divergence of transcriptional programs between SG and MP in response to WS exemplifies the two different stress-response strategies of these grapevine cultivars.

In accordance with the previous findings in the original reference publication [15], our research identified the activation of genes coding for chaperones and heat-shock proteins

in response to prolonged WS. Chaperones and heat-shock proteins are crucial components of the cell's machinery for protein folding. They assist in the proper folding of proteins and prevent the aggregation of misfolded proteins, which can be detrimental to cellular function and survival. Under normal conditions, proteins fold into their functional, three-dimensional structures with the help of chaperones. However, under stress conditions like drought, the normal protein folding process can be disrupted, leading to the accumulation of misfolded or unfolded proteins. Hence, the activation of genes coding for chaperones and heat-shock proteins is a critical component of the plant's response to long-lasting WS.

Our trajectory analysis based on module activation adds a novel, more comprehensive view of WS dynamics in the anisohydric and isohydric cultivars not addressed by Dal Santo and colleagues [15]. SOM portrayal reveals that during the initial stages of water deprivation, both vine cultivars adjust the cell wall composition and structure that might be necessary to cope with reduced water availability. This suggests that it starts with physical reinforcement of the cell wall, followed by broader stress signaling and adjustment, and finally, adaptation for long-term survival through compatible solutes and protein stability. This could help the grapevine to maintain cell integrity under the pressure of water deficit, reduce water loss by creating a tighter barrier, and enhance resistance to potential secondary stresses like pathogens that might exploit drought-weakened plants. The activation of specific transcription factors like MYB, WRKY, and AS2 signifies a shift towards a broader stress response. We speculate that the WS-driven upregulation of steroid and lipid biosynthesis, specifically in anisohydric SG, strengthens cell membranes, while ketoreductases help detoxify harmful substances. This response also involves the production of phytohormones, like ABA and antioxidants, to protect cells from damage.

On the other hand, the isohydric MP prevails in water conservation and stomatal regulation, which diminishes water loss under WS. The stilbenoids, diarylheptanoids, and gingerols possess antioxidant properties so they could mitigate oxidative stress induced by drought. The isohydric vine may allocate resources towards a synthesis of such compounds to bolster the defense mechanisms against drought-induced oxidative stress and enhance tolerance to water deficit.

Moreover, our analysis indicates fast activation of stilbenoid biosynthesis genes (*C4H*, *RS*, *ROMT*, promiscuous *HCT*, and *CCoAOMT*) in the isohydric grape cultivar under WS. Particularly, the increased expression of resveratrol biosynthesis genes in MP (compared to SG) implies that wines derived from this cultivar may accumulate higher resveratrol content than those from the SG cultivar under WS conditions.

In our previous work, we identified the upregulation of thiamine biosynthetic genes in low- and extremely low-temperature stress [18], which motivated us to analyze this pathway under WS. Notably, recent studies have highlighted the significance of thiamine in the plant response to WS [70,71], demonstrating significant upregulation of *THI1* and *THIC* genes under drought and dry air humidity stresses [72,73]. Our findings support the hypothesis that the production of thiamine is not only a cold acclimation stress-responsive but also a WS-responsive compound in both iso- and aniso-hydric vine cultivars. Here, we provided more elaborate insights into the cascade of gene activation underlying stress response mechanisms in grapevine.

The focus on stilbenoid and thiamine pathways is, although justified by the data and motivated by our previous work, somewhat arbitrary, but it illustrates the potency of the transcriptomic data for extracting WS responses at the pathway level. Although their phenotypes assign them isohydric and anisohydric characteristics, differential gene expression between them does not necessarily directly relate to molecular causes of the different water management strategies. Future investigations should generalize the results by extending the number of vine accessions in similar experimental and analysis settings.

In conclusion, the dynamics of biological processes in both studied cultivars under WS and control conditions might shed light on further vine research. Experimental studies are needed to fully understand these mechanisms and their potential applications in improving drought resistance, which has significant implications for vine production, particularly in

regions where water availability is a major constraint. In the future, this research might help to explore the possibility of manipulating biochemical pathways to enhance drought tolerance in other vine cultivars, securing viticulture in the face of changing climate. Overall, our findings underscore the genomic diversity and different adaptability of these cultivars to changing environments.

4. Materials and Methods

4.1. Expression Data and Treatment Conditions

The gene expression data were downloaded from the supporting dataset (GEO: GSE70670; <http://www.ncbi.nlm.nih.gov/geo/query/acc.cgi?token=ovqbgaqedfaxjqn&acc=GSE70670>; accessed on 3 February 2024) provided by Dal Santo and colleagues [15]. It encompasses normalized gene expression data (NimbleScan v2.5 software-calculated Robust Multiarray Average/RMA-normalized signal intensities) from leaves (L) of two grapevine (*Vitis vinifera* L.) cultivars, ‘Montepulciano’—clone R7 (here referred to as MP) and ‘Sangiovese’—clone VCR30 (here referred to as SG), possessing isohydric and anisohydric characteristics, respectively. For a detailed description of the experimental set-up, we refer to the original publication [15]. In short, both cultivars were grafted onto 1103 Paulsen rootstock, and 8-year-old, well-maintained, greenhouse-potted vines were used in the experiment. Two groups were established for each cultivar: a water-stressed group (STRS) that received 40% of maximum water availability relative to the soil field capacity of 30.2% [(vol water/vol soil) × 100], and a well-watered control group (CTRL) that received 90% of maximum water availability. The samples were collected for the analysis of transcriptome at three time points following the initiation of WS: 2, 6, and 27 days (referred to as T1, T2, and T3, respectively). These time points represent different stages of drought stress, ranging from the initial onset of WS to prolonged exposure to the stress. The experiment included three biological replicates (r1, r2, and r3) for each condition in both cultivars. Dal Santo and colleagues complemented transcriptomic measurement with phenotypic data, particularly leaf physiological and leaf biochemical parameters. We refer to the original publication for details [15].

4.2. Self-Organizing Map

The SOM portrayal algorithm was employed to analyze the preprocessed gene expression data using the oposSOM software (version 2.2.5), as described previously [18]. A total of 36 samples were used as input, containing expression values for 28,521 genes. These represent 81.18% of the 35,134 annotated coding genes of *Vitis vinifera* that were found in the Ensembl database [74,75] on the 16th of May, 2023. The SOM was configured to have 1600 neurons (also called metagenes, characterizing the mean transcriptional profile of the genes collected in the respective neuron), arranged in a quadratic lattice with dimensions 40×40 . During training, the SOM distributed the gene expression values across the neurons/metagenes, effectively reducing the high-dimensional data into a 2-dimensional representation. The gene expression profiles of each treatment condition, including control and stressed samples for both cultivars, were mapped onto the SOM grid. The resulting SOM, obtained for each treatment condition, was visualized as an expression “portrait”. To enable the visual interpretation of these SOM “portraits”, a tertiary color code was used to color each metagene, ranging from red through green to blue, corresponding to high to low gene expression. As the metagenes that are located close to each other include genes with similar expression profiles, we can define red and blue spots in the SOM “portraits”. Red spots signify transcript upregulation, while blue spots indicate transcript downregulation, deviating more than the upper or lower quartile in a positive or negative direction, respectively.

Alternatively, we used “waterline” profiles, indicating expression values above and below the mean in red and blue, respectively, to better visualize slight changes in the transcriptome patterns. Statistics of the spot expression in terms of jointly activated spots in the individual portraits, spot number frequencies, and mean numbers of spots per portrait

provide details of the topology of the activated transcriptome under the different treatment conditions. For a comparison of differentially expressed genes published in the previous study [15] with our SOM results, we mapped the selected marker genes into our SOM expression landscape to show their distribution (see Figures A1–A4). The sample similarity analysis uses a pairwise correlation map, independent component analysis, and sample SOM presentations. Details of the methods used and their applications to different use cases were described previously [20,64–66] and are available in the R-package oposSOM [62].

4.3. Functional Annotation

KEGG [76] and VitisNet [77] databases were used to functionally annotate genes for the gene set analysis, and PANTHER (version 18.0; [78]) was employed with default settings for the gene ontology (GO) enrichment analysis (for details see [18]). Genes from the KEGG pathways mentioned in this work were mapped onto SOM overexpression spots.

Author Contributions: Conceptualization, A.A., H.B. and T.K.; methodology, A.A., T.K., H.B. and M.N.; validation, A.A., T.K., H.B. and M.N.; formal analysis, T.K., H.B. and A.A.; investigation, A.A., T.K. and H.B.; resources, A.A. and T.K.; data curation, A.A. and T.K.; writing—original draft preparation, A.A., T.K. and H.B.; writing—review and editing, A.A., T.K. and H.B.; visualization, T.K.; supervision, H.B.; project administration, H.B.; funding acquisition, H.B. All authors have read and agreed to the published version of the manuscript.

Funding: This work was supported by the Foundation of Armenian Science and Technology (FAST) within the framework of the ADVANCE Research Grants Program project Vine Bioinformatics—grape genomics for innovative viticulture, funded by Joe Barnes. We acknowledge financial support from the German Research Foundation (DFG) and Universität Leipzig within the program of Open Access Publishing.

Data Availability Statement: Expression data were taken from a previous study [15]. The R-object of our SOM analysis is deposited online in the Leipzig Health Atlas with the accession number 611 (LHA:611; https://www.health-atlas.de/data_files/611 accessed on 26 July 2024).

Conflicts of Interest: The authors declare no conflicts of interest.

Appendix A

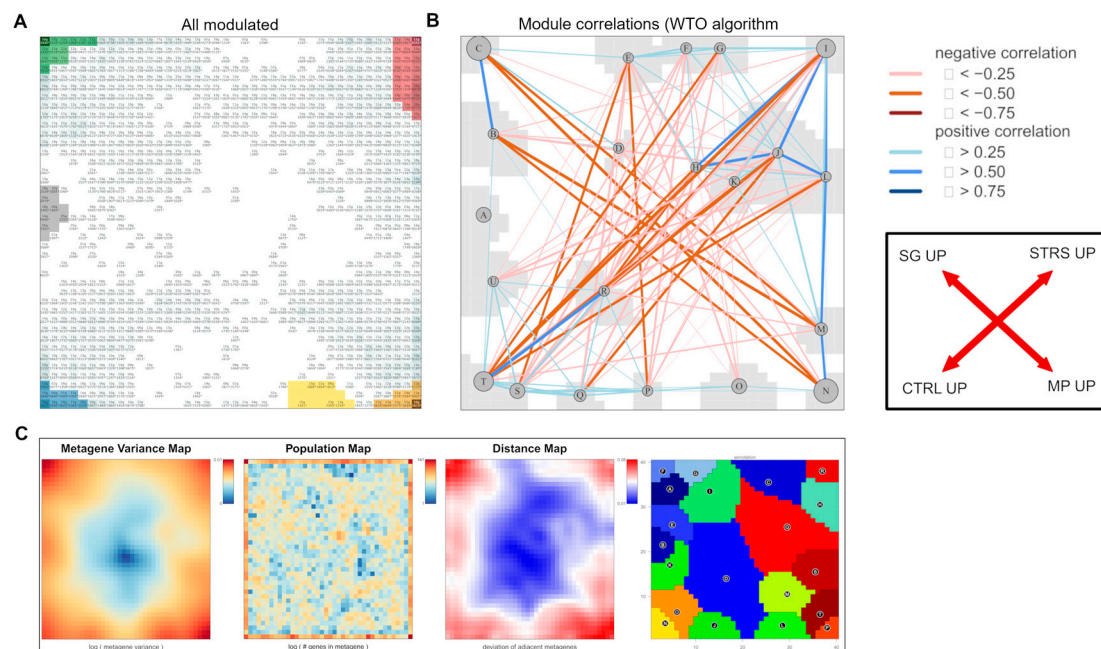


Figure A1. Covariance and population structure of the SOM expression landscape. (A) The 5947 genes significantly modulated in leaves under our experimental conditions were taken from the SAM analysis

in [15] and mapped into our SOM. Occupied metagenes (pixels) are marked in greyish. They refer mostly to metagenes of high and moderate variance of gene expression (see part C). (B) The covariance structure of the SOM was estimated by calculating a weighted topological overlap (WTO) network between the spot modules [65]. It reveals strong anticorrelations ($w < 0$) between the two cultivars (SG vs. MP) and between the two conditions (STRS vs. CTRL; see the scheme on the right). It thus assigns the “modulated genes” (part A) to up- and downregulation under the different conditions. Note also that the SOM decomposes the “modulated genes” into clusters of co-regulated genes called spot modules. (C) The variance map of the metagenes reveals a variance gradient of gene expression from the center of the SOM (blue) towards its edges (brown). The population map color codes the number of genes per metagene from high (red) to low (blue). The gene density changes across the SOM. Also, the Euclidean distances between neighboring metagenes are variant and “amplify” regions of increased gene density. The K-means map provides a space-filling segmentation of the SOM, enabling it to consider any region for downstream analysis, such as function mining.

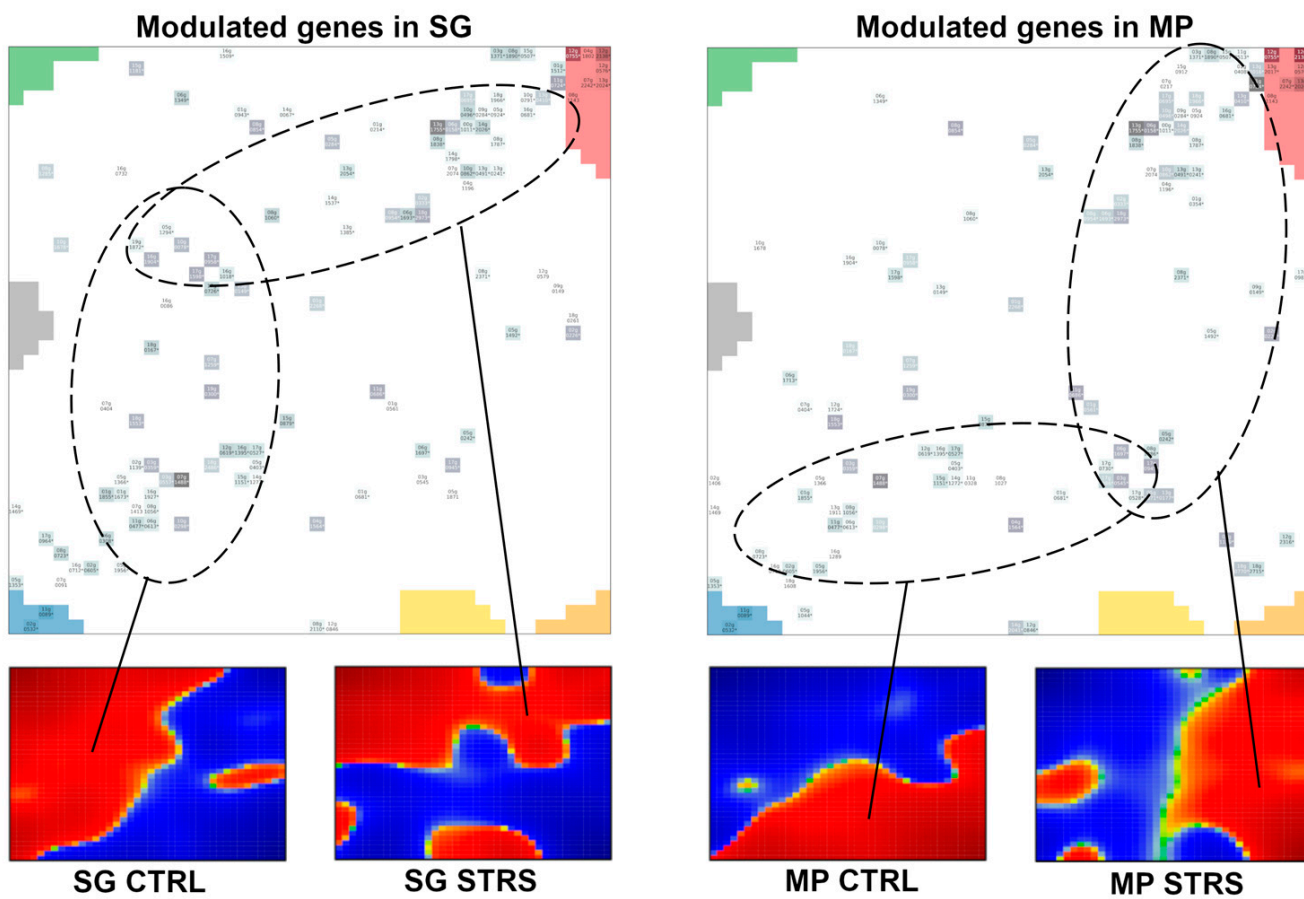


Figure A2. Genes specifically modulated in the accessions were taken from supporting data [15] and compared to the respective waterline portraits. Genes modulated in SG and MP accumulate in the overexpressed areas in SG and MP, respectively.

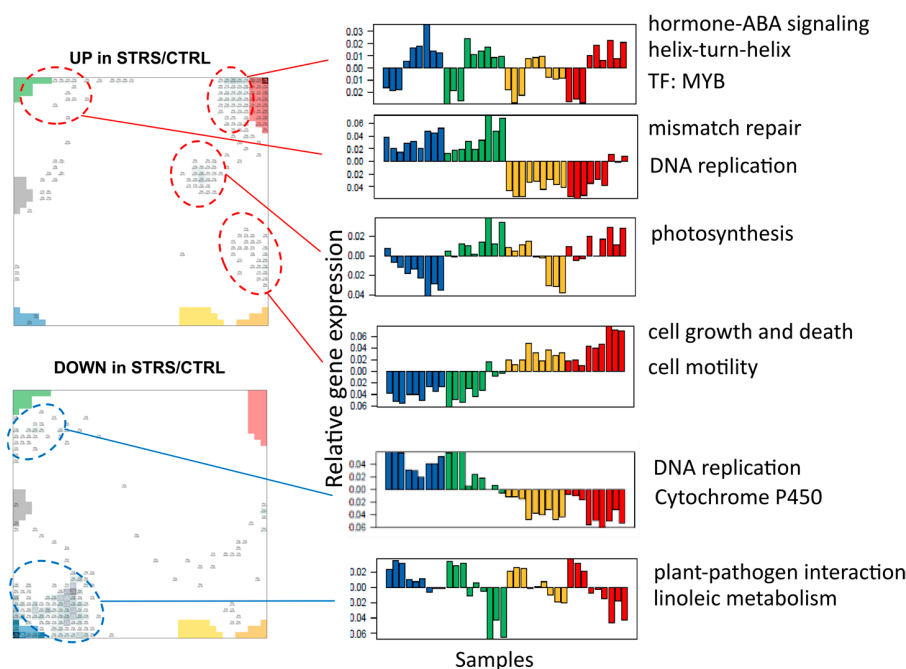


Figure A3. Genes modulated specifically under stress conditions. The cutoffs defining upregulated (UP in STRS/CTRL) and downregulated (DOWN in STRS/CTRL) genes were taken from [15] (fold change > 2 and top 20% variant genes) and mapped into the SOM. Clusters of genes accumulate in different areas of the SOM in and near the spots. The respective profiles are shown on the right, together with the respective biological functions. As expected, the profiles confirm the UP/DOWN under STRS conditions, showing the respective changes, especially under lasting stress at T3. The profiles also show that the expression changes are about one order of magnitude smaller compared with that observed in the spots. The bars are color-coded as in the other figures.

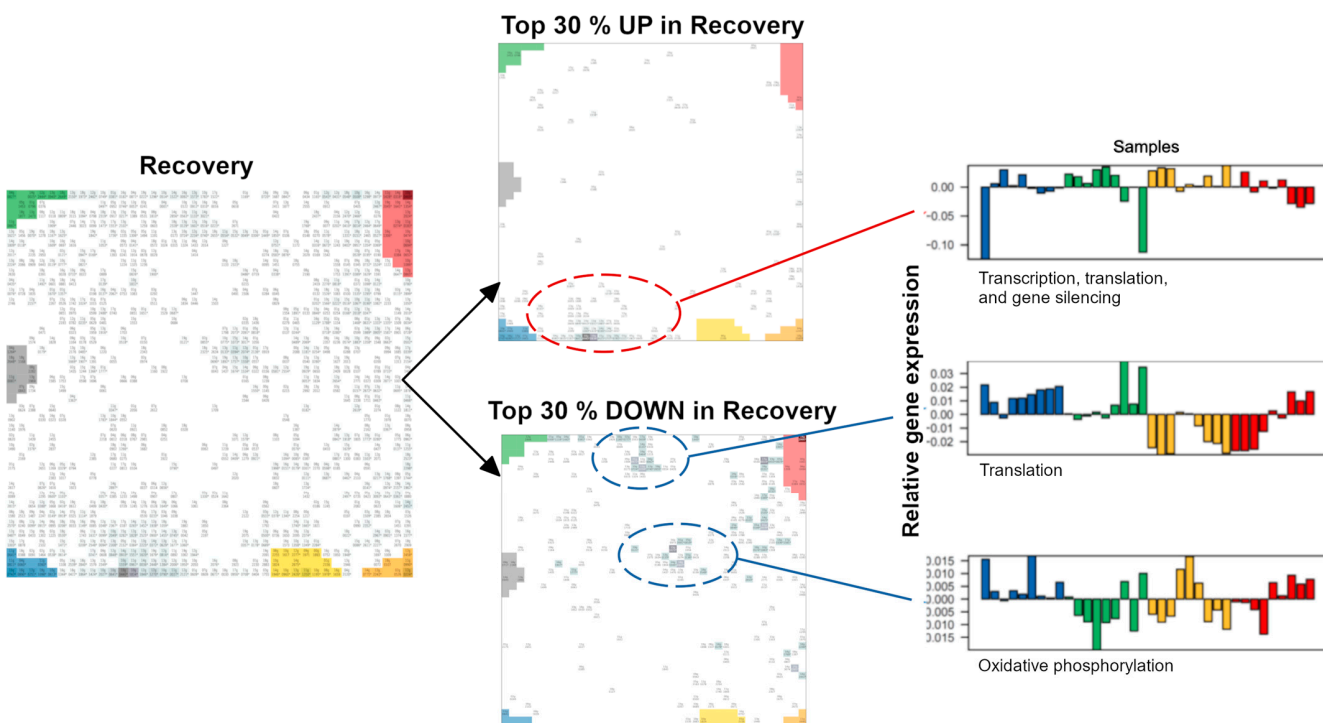


Figure A4. Genes specifically modulated under recovery from WS. Recovery conditions were achieved by re-watering the plants 46 days after the onset of WS, and the post-recovery plant material

was collected 70 days after the onset of WS (see Materials and Methods in [15]). Upregulated (UP) and downregulated (DOWN) genes and their respective profiles are shown separately. The profiles refer to the stress experiment. Recovery virtually reverses expression changes observed for lasting stress (STRS at T3).

Table A1. Lists of genes in the SOM spots A–F. Number of genes per each spot is in parentheses.

A (376 Genes)	B (309 Genes)	C (340 Genes)	D (384 Genes)	E (462 Genes)	F (695 Genes)
Vitvi17g00237	Vitvi10g02124	Vitvi15g01586	Vitvi04g02074	Vitvi14g02553	Vitvi13g00164
Vitvi16g01025	Vitvi08g01847	Vitvi18g00424	Vitvi04g00410	Vitvi09g01725	Vitvi06g01513
Vitvi01g00437	Vitvi10g02194	Vitvi10g00667	Vitvi18g02126	Vitvi13g02480	Vitvi13g00169
Vitvi01g00580	Vitvi18g02451	Vitvi15g01587	Vitvi18g00833	Vitvi19g02069	Vitvi12g00573
Vitvi01g01028	Vitvi05g01951	Vitvi10g01684	Vitvi01g01736	Vitvi17g01664	Vitvi07g02152
Vitvi19g00388	Vitvi10g02121	Vitvi04g00501	Vitvi19g00456	Vitvi07g02304	Vitvi14g01193
Vitvi18g02718	Vitvi07g00973	Vitvi05g01760	Vitvi04g02122	Vitvi10g00867	Vitvi19g00618
Vitvi14g01657	Vitvi17g01737	Vitvi13g01250	Vitvi19g01484	Vitvi09g01261	Vitvi13g00166
Vitvi14g02664	Vitvi17g01732	Vitvi11g00016	Vitvi02g01517	Vitvi04g02117	Vitvi13g00471
Vitvi15g01691	Vitvi10g02195	Vitvi01g01917	Vitvi18g00596	Vitvi17g01693	Vitvi13g00162
Vitvi16g01878	Vitvi08g01380	Vitvi15g00970	Vitvi05g01287	Vitvi16g01659	Vitvi04g01974
Vitvi04g00827	Vitvi13g00925	Vitvi07g02119	Vitvi19g01674	Vitvi16g00770	Vitvi07g00055
Vitvi07g01789	Vitvi17g01736	Vitvi06g00268	Vitvi10g01493	Vitvi04g01870	Vitvi05g01933
Vitvi03g01162	Vitvi10g02181	Vitvi07g02123	Vitvi08g01548	Vitvi18g02894	Vitvi06g00526
Vitvi18g00871	Vitvi04g01325	Vitvi16g00941	Vitvi16g00027	Vitvi01g02297	Vitvi18g01438
Vitvi17g01541	Vitvi10g02190	Vitvi18g01937	Vitvi07g02288	Vitvi07g02725	Vitvi09g01282
Vitvi18g02157	Vitvi12g00224	Vitvi15g00714	Vitvi03g01582	Vitvi14g02863	Vitvi10g00034
Vitvi16g02001	Vitvi18g02293	Vitvi01g01934	Vitvi15g01364	Vitvi14g01112	Vitvi18g02423
Vitvi02g01350	Vitvi11g00460	Vitvi02g01404	Vitvi13g02086	Vitvi18g02584	Vitvi10g01778
Vitvi04g01352	Vitvi04g02105	Vitvi07g01844	Vitvi13g02044	Vitvi19g01302	Vitvi07g00259
Vitvi13g01356	Vitvi18g02289	Vitvi18g01263	Vitvi10g01807	Vitvi14g01082	Vitvi13g02077
Vitvi05g01256	Vitvi06g01097	Vitvi18g02446	Vitvi10g00859	Vitvi14g01106	Vitvi08g00731
Vitvi08g01052	Vitvi00g00339	Vitvi04g00760	Vitvi10g02180	Vitvi14g01080	Vitvi18g01070
Vitvi19g01504	Vitvi16g01302	Vitvi15g01582	Vitvi15g00736	Vitvi16g01613	Vitvi02g01447
Vitvi12g02444	Vitvi18g03097	Vitvi02g01403	Vitvi14g03039	Vitvi17g01674	Vitvi07g00455
Vitvi18g03185	Vitvi19g00216	Vitvi10g00742	Vitvi17g00315	Vitvi15g01363	Vitvi01g02273
Vitvi12g02069	Vitvi12g00602	Vitvi05g00011	Vitvi19g01322	Vitvi14g02865	Vitvi18g02559
Vitvi19g01984	Vitvi04g01233	Vitvi18g02287	Vitvi14g02789	Vitvi19g02154	Vitvi10g00403
Vitvi01g00350	Vitvi04g01375	Vitvi03g01621	Vitvi18g01927	Vitvi14g02533	Vitvi19g02371
Vitvi14g02925	Vitvi14g00297	Vitvi14g00500	Vitvi04g00160	Vitvi16g02162	Vitvi06g01575
Vitvi19g00107	Vitvi13g01320	Vitvi06g01604	Vitvi08g02076	Vitvi08g01978	Vitvi02g00020
Vitvi01g01982	Vitvi02g00783	Vitvi06g01601	Vitvi13g00109	Vitvi14g01075	Vitvi14g03078
Vitvi12g00927	Vitvi08g02249	Vitvi02g00393	Vitvi16g01641	Vitvi14g02548	Vitvi05g00139
Vitvi18g00717	Vitvi12g02165	Vitvi14g01381	Vitvi18g03208	Vitvi14g01096	Vitvi19g00381
Vitvi17g00609	Vitvi04g01940	Vitvi03g00708	Vitvi09g01460	Vitvi16g00772	Vitvi05g00681
Vitvi15g00005	Vitvi06g01100	Vitvi07g01697	Vitvi14g03080	Vitvi10g01046	Vitvi06g01746
Vitvi00g01279	Vitvi05g02283	Vitvi05g02248	Vitvi08g01941	Vitvi06g01301	Vitvi12g00301
Vitvi11g00526	Vitvi10g02113	Vitvi18g02727	Vitvi07g02115	Vitvi10g01626	Vitvi16g00205
Vitvi02g01806	Vitvi07g02402	Vitvi11g01674	Vitvi12g02456	Vitvi12g02239	Vitvi11g01450
Vitvi03g01891	Vitvi09g01214	Vitvi18g00979	Vitvi01g01387	Vitvi10g00869	Vitvi09g00246
Vitvi10g02223	Vitvi05g00669	Vitvi18g02592	Vitvi07g02146	Vitvi09g00878	Vitvi11g01333
Vitvi10g00001	Vitvi13g01889	Vitvi19g00094	Vitvi08g02329	Vitvi18g03390	Vitvi11g00251
Vitvi12g02448	Vitvi18g02463	Vitvi12g02244	Vitvi08g01303	Vitvi13g02426	Vitvi10g00459
Vitvi08g01404	Vitvi15g01669	Vitvi11g01491	Vitvi19g02218	Vitvi13g01559	Vitvi14g01951
Vitvi08g01617	Vitvi02g01037	Vitvi05g01577	Vitvi04g02233	Vitvi18g03068	Vitvi05g00461
Vitvi14g01127	Vitvi13g01404	Vitvi14g01868	Vitvi14g02756	Vitvi18g02935	Vitvi16g01985
Vitvi13g01180	Vitvi15g01663	Vitvi07g02735	Vitvi18g01565	Vitvi16g01469	Vitvi12g02469
Vitvi11g01251	Vitvi01g00555	Vitvi09g01536	Vitvi04g00988	Vitvi00g02157	Vitvi03g00119
Vitvi14g02469	Vitvi16g02010	Vitvi14g01488	Vitvi12g01676	Vitvi18g02870	Vitvi04g02187
Vitvi05g02198	Vitvi10g02119	Vitvi15g00844	Vitvi17g00662	Vitvi14g02864	Vitvi19g02000
Vitvi17g00788	Vitvi18g02631	Vitvi02g00391	Vitvi08g00199	Vitvi18g03332	Vitvi00g02173
Vitvi14g02722	Vitvi10g02301	Vitvi06g01515	Vitvi08g02328	Vitvi01g01614	Vitvi12g00028

Table A1. Cont.

A (376 Genes)	B (309 Genes)	C (340 Genes)	D (384 Genes)	E (462 Genes)	F (695 Genes)
Vitvi03g01584	Vitvi05g01940	Vitvi07g00665	Vitvi13g02029	Vitvi09g00908	Vitvi18g02906
Vitvi01g00605	Vitvi14g02575	Vitvi14g02913	Vitvi18g03011	Vitvi14g01113	Vitvi08g02117
Vitvi03g01890	Vitvi16g01449	Vitvi08g02147	Vitvi10g01983	Vitvi13g00931	Vitvi07g00293
Vitvi04g02192	Vitvi17g00972	Vitvi01g01921	Vitvi02g01439	Vitvi16g01474	Vitvi19g01760
Vitvi17g00639	Vitvi18g02464	Vitvi09g00264	Vitvi05g00716	Vitvi04g02121	Vitvi08g02393
Vitvi03g01603	Vitvi08g01848	Vitvi12g02565	Vitvi09g00524	Vitvi17g00592	Vitvi02g00543
Vitvi18g02061	Vitvi10g01613	Vitvi12g02718	Vitvi08g02343	Vitvi13g02424	Vitvi05g01837
Vitvi18g02716	Vitvi18g02273	Vitvi07g02114	Vitvi19g02019	Vitvi08g00035	Vitvi04g01794
Vitvi17g00405	Vitvi10g02174	Vitvi18g03084	Vitvi14g02445	Vitvi18g01019	Vitvi04g01920
Vitvi14g01222	Vitvi02g01850	Vitvi02g01440	Vitvi18g02586	Vitvi16g01481	Vitvi19g02268
Vitvi05g01439	Vitvi12g02275	Vitvi08g00768	Vitvi18g00164	Vitvi18g02881	Vitvi02g00264
Vitvi00g02337	Vitvi12g02241	Vitvi11g00726	Vitvi14g00940	Vitvi12g02350	Vitvi14g01726
Vitvi01g00065	Vitvi18g03265	Vitvi01g00710	Vitvi14g02691	Vitvi09g02069	Vitvi07g02229
Vitvi03g01887	Vitvi12g02245	Vitvi07g02604	Vitvi12g02386	Vitvi16g01457	Vitvi19g01791
Vitvi08g00942	Vitvi07g02390	Vitvi07g02650	Vitvi09g00304	Vitvi00g02261	Vitvi14g01942
Vitvi13g02451	Vitvi12g02243	Vitvi08g01291	Vitvi04g00013	Vitvi12g02338	Vitvi02g00162
Vitvi12g01836	Vitvi12g02274	Vitvi11g00467	Vitvi09g01984	Vitvi12g02340	Vitvi08g01656
Vitvi18g02722	Vitvi18g03098	Vitvi14g01815	Vitvi18g02521	Vitvi16g01702	Vitvi13g01839
Vitvi12g00596	Vitvi11g01701	Vitvi14g00461	Vitvi07g01519	Vitvi16g00133	Vitvi05g01839
Vitvi01g00697	Vitvi01g00532	Vitvi06g00931	Vitvi19g00604	Vitvi15g01406	Vitvi07g00117
Vitvi07g01990	Vitvi11g01037	Vitvi05g00710	Vitvi07g02322	Vitvi12g01852	Vitvi01g00329
Vitvi04g02196	Vitvi02g01649	Vitvi19g00321	Vitvi12g02387	Vitvi09g00920	Vitvi08g02274
Vitvi14g01149	Vitvi13g00701	Vitvi14g02930	Vitvi15g01372	Vitvi11g00126	Vitvi16g01022
Vitvi12g02742	Vitvi08g01650	Vitvi18g00675	Vitvi04g02129	Vitvi13g01566	Vitvi13g02070
Vitvi19g00656	Vitvi07g01308	Vitvi09g00233	Vitvi10g02222	Vitvi19g02190	Vitvi07g01296
Vitvi12g00036	Vitvi12g02292	Vitvi14g00483	Vitvi07g02949	Vitvi18g02746	Vitvi14g01354
Vitvi03g00406	Vitvi05g01934	Vitvi01g00784	Vitvi06g00040	Vitvi09g00907	Vitvi06g01360
Vitvi12g00478	Vitvi12g00243	Vitvi15g00314	Vitvi04g00467	Vitvi16g00761	Vitvi07g00380
Vitvi12g01984	Vitvi12g02285	Vitvi16g01213	Vitvi17g00895	Vitvi06g01812	Vitvi05g00857
Vitvi12g02569	Vitvi19g02111	Vitvi04g00442	Vitvi03g01521	Vitvi07g02369	Vitvi13g02192
Vitvi14g01952	Vitvi09g01872	Vitvi13g00509	Vitvi13g00546	Vitvi09g01782	Vitvi09g01904
Vitvi16g01697	Vitvi10g01656	Vitvi14g01977	Vitvi14g02916	Vitvi16g00251	Vitvi08g02143
Vitvi09g01145	Vitvi01g00574	Vitvi06g01597	Vitvi13g01737	Vitvi13g01564	Vitvi10g00330
Vitvi06g00714	Vitvi17g01739	Vitvi02g01661	Vitvi16g01122	Vitvi14g02773	Vitvi18g01510
Vitvi07g00130	Vitvi03g01777	Vitvi06g00790	Vitvi07g03080	Vitvi16g01464	Vitvi00g02264
Vitvi08g01333	Vitvi07g02231	Vitvi18g00967	Vitvi09g00700	Vitvi16g00991	Vitvi08g01543
Vitvi05g01151	Vitvi06g01577	Vitvi04g02241	Vitvi06g00894	Vitvi18g03026	Vitvi16g01144
Vitvi17g00175	Vitvi18g02508	Vitvi18g00956	Vitvi14g02449	Vitvi09g01663	Vitvi19g02274
Vitvi15g01651	Vitvi18g00290	Vitvi18g00476	Vitvi14g00958	Vitvi03g01749	Vitvi13g00490
Vitvi19g02029	Vitvi04g01241	Vitvi08g01335	Vitvi01g02264	Vitvi17g01665	Vitvi13g00688
Vitvi14g02515	Vitvi03g01885	Vitvi13g00114	Vitvi14g01939	Vitvi14g02570	Vitvi05g00118
Vitvi12g02454	Vitvi09g01187	Vitvi10g01615	Vitvi09g00560	Vitvi02g01072	Vitvi08g02015
Vitvi16g02146	Vitvi12g02289	Vitvi11g01488	Vitvi10g01009	Vitvi19g01220	Vitvi17g00554
Vitvi07g00021	Vitvi07g01814	Vitvi16g01931	Vitvi15g01257	Vitvi12g02345	Vitvi08g00656
Vitvi02g00171	Vitvi16g02005	Vitvi08g00630	Vitvi07g00781	Vitvi14g00218	Vitvi10g00558
Vitvi18g01884	Vitvi03g01896	Vitvi02g01459	Vitvi13g00556	Vitvi05g01039	Vitvi05g01392
Vitvi10g01650	Vitvi15g01762	Vitvi16g01932	Vitvi18g02673	Vitvi18g02889	Vitvi04g01793
Vitvi17g01414	Vitvi12g02269	Vitvi08g01702	Vitvi09g00708	Vitvi07g02079	Vitvi07g00256
Vitvi04g01815	Vitvi12g01121	Vitvi19g00404	Vitvi08g01625	Vitvi05g02015	Vitvi06g00999
Vitvi14g03033	Vitvi17g01302	Vitvi19g00690	Vitvi14g02736	Vitvi14g02550	Vitvi09g00996
Vitvi14g01211	Vitvi08g01382	Vitvi18g01938	Vitvi03g01556	Vitvi07g02387	Vitvi05g00204
Vitvi07g00586	Vitvi08g02247	Vitvi04g01481	Vitvi04g02014	Vitvi19g01921	Vitvi09g00275
Vitvi04g00282	Vitvi05g02086	Vitvi18g01001	Vitvi07g01653	Vitvi16g01473	Vitvi07g03183
Vitvi18g01895	Vitvi10g02106	Vitvi14g01739	Vitvi01g00291	Vitvi16g01570	Vitvi12g00444
Vitvi01g00319	Vitvi00g01453	Vitvi11g00641	Vitvi10g01994	Vitvi14g02828	Vitvi05g01840
Vitvi18g02320	Vitvi04g01890	Vitvi03g01276	Vitvi07g00843	Vitvi19g00423	Vitvi14g01943
Vitvi00g00342	Vitvi12g00610	Vitvi08g01701	Vitvi18g02791	Vitvi12g02277	Vitvi08g01532
Vitvi01g01884	Vitvi18g00860	Vitvi09g00971	Vitvi13g00635	Vitvi19g02228	Vitvi02g00263

Table A1. Cont.

A (376 Genes)	B (309 Genes)	C (340 Genes)	D (384 Genes)	E (462 Genes)	F (695 Genes)
Vitvi17g01393	Vitvi14g02609	Vitvi05g00094	Vitvi07g01638	Vitvi18g01447	Vitvi05g00430
Vitvi16g01566	Vitvi19g00445	Vitvi10g01734	Vitvi11g00914	Vitvi15g01326	Vitvi12g00462
Vitvi07g01720	Vitvi12g02702	Vitvi10g00436	Vitvi18g01056	Vitvi18g01442	Vitvi07g02212
Vitvi16g00908	Vitvi01g02003	Vitvi19g02050	Vitvi18g00241	Vitvi12g02617	Vitvi14g00971
Vitvi12g02080	Vitvi10g02129	Vitvi09g01399	Vitvi10g00938	Vitvi12g02337	Vitvi07g00598
Vitvi13g00025	Vitvi01g00611	Vitvi01g00525	Vitvi04g00570	Vitvi15g01680	Vitvi17g00116
Vitvi17g00358	Vitvi05g02215	Vitvi09g01616	Vitvi07g02462	Vitvi05g02038	Vitvi06g00561
Vitvi06g01093	Vitvi12g02238	Vitvi10g02351	Vitvi11g01323	Vitvi08g02128	Vitvi03g00206
Vitvi08g01403	Vitvi13g01312	Vitvi15g01355	Vitvi09g01966	Vitvi13g02355	Vitvi19g02012
Vitvi19g01503	Vitvi04g01519	Vitvi17g00804	Vitvi17g00119	Vitvi19g01313	Vitvi05g01842
Vitvi18g03070	Vitvi12g02273	Vitvi03g00325	Vitvi02g01703	Vitvi06g01980	Vitvi11g00389
Vitvi13g00026	Vitvi19g00424	Vitvi05g00544	Vitvi17g01599	Vitvi14g02818	Vitvi12g02668
Vitvi19g00525	Vitvi14g02594	Vitvi11g00243	Vitvi16g01630	Vitvi18g03324	Vitvi14g00038
Vitvi03g00482	Vitvi19g01884	Vitvi06g00303	Vitvi02g00042	Vitvi09g00924	Vitvi08g01777
Vitvi11g00528	Vitvi05g01943	Vitvi07g02605	Vitvi15g00206	Vitvi03g00976	Vitvi17g00617
Vitvi16g02105	Vitvi00g01462	Vitvi16g01980	Vitvi07g01693	Vitvi05g01181	Vitvi03g00164
Vitvi10g00164	Vitvi16g01251	Vitvi09g01694	Vitvi08g01439	Vitvi16g00749	Vitvi13g00062
Vitvi02g00056	Vitvi13g00702	Vitvi10g00787	Vitvi08g01047	Vitvi18g03058	Vitvi17g00778
Vitvi12g00598	Vitvi00g01457	Vitvi04g00960	Vitvi19g02100	Vitvi11g01574	Vitvi04g01368
Vitvi04g02198	Vitvi06g00379	Vitvi11g01676	Vitvi19g02077	Vitvi17g01680	Vitvi05g01834
Vitvi01g00822	Vitvi19g01685	Vitvi17g01467	Vitvi04g01583	Vitvi05g01861	Vitvi05g01841
Vitvi09g00790	Vitvi18g03280	Vitvi08g01384	Vitvi10g00881	Vitvi19g01043	Vitvi03g01391
Vitvi19g00205	Vitvi12g02433	Vitvi10g01616	Vitvi17g00605	Vitvi14g02547	Vitvi18g01545
Vitvi18g00764	Vitvi14g00896	Vitvi01g00567	Vitvi12g00491	Vitvi16g01591	Vitvi06g00440
Vitvi14g00103	Vitvi12g00334	Vitvi07g03053	Vitvi05g01838	Vitvi09g00912	Vitvi08g00125
Vitvi09g01979	Vitvi14g02924	Vitvi18g02835	Vitvi19g01305	Vitvi09g00894	Vitvi08g01843
Vitvi05g02009	Vitvi17g01731	Vitvi10g02034	Vitvi10g01014	Vitvi16g01619	Vitvi04g00135
Vitvi19g01817	Vitvi14g02759	Vitvi13g00870	Vitvi08g02259	Vitvi13g01445	Vitvi02g00395
Vitvi12g00554	Vitvi12g02272	Vitvi07g01739	Vitvi01g01912	Vitvi15g01321	Vitvi05g02185
Vitvi13g01904	Vitvi02g01832	Vitvi06g00317	Vitvi18g02806	Vitvi14g02543	Vitvi08g02412
Vitvi07g00810	Vitvi15g00107	Vitvi17g01691	Vitvi17g01105	Vitvi18g03041	Vitvi10g00474
Vitvi01g00585	Vitvi11g00990	Vitvi13g01389	Vitvi13g02337	Vitvi07g02362	Vitvi14g00318
Vitvi19g01883	Vitvi09g01673	Vitvi08g01221	Vitvi11g00498	Vitvi09g01465	Vitvi02g00505
Vitvi03g01886	Vitvi14g03049	Vitvi03g00251	Vitvi16g00808	Vitvi10g01301	Vitvi15g00511
Vitvi01g00320	Vitvi00g01467	Vitvi04g00486	Vitvi03g01481	Vitvi14g02544	Vitvi18g01131
Vitvi19g01819	Vitvi11g01222	Vitvi04g00510	Vitvi13g01790	Vitvi13g02078	Vitvi15g00816
Vitvi13g02187	Vitvi07g02710	Vitvi10g00613	Vitvi01g00260	Vitvi13g02275	Vitvi01g00745
Vitvi19g00522	Vitvi16g01531	Vitvi16g00401	Vitvi13g01862	Vitvi03g01736	Vitvi03g00024
Vitvi07g03077	Vitvi18g02844	Vitvi11g00098	Vitvi01g02287	Vitvi11g01249	Vitvi13g02457
Vitvi19g00565	Vitvi16g00913	Vitvi19g00218	Vitvi18g03359	Vitvi06g01157	Vitvi10g01237
Vitvi19g01893	Vitvi05g01229	Vitvi13g00172	Vitvi14g01937	Vitvi03g01738	Vitvi03g01746
Vitvi13g02505	Vitvi09g00889	Vitvi02g00564	Vitvi06g01975	Vitvi18g02945	Vitvi11g00518
Vitvi12g00330	Vitvi12g02240	Vitvi16g00282	Vitvi18g01065	Vitvi18g03349	Vitvi02g01270
Vitvi03g01593	Vitvi14g01681	Vitvi10g01840	Vitvi14g01508	Vitvi04g01050	Vitvi08g01391
Vitvi06g00310	Vitvi09g01798	Vitvi18g01705	Vitvi14g02809	Vitvi14g03083	Vitvi14g00156
Vitvi01g00399	Vitvi16g01894	Vitvi11g00099	Vitvi03g01863	Vitvi10g01988	Vitvi13g02073
Vitvi08g01032	Vitvi10g02167	Vitvi01g01751	Vitvi12g02413	Vitvi16g02163	Vitvi03g00586
Vitvi19g00586	Vitvi13g01006	Vitvi13g01913	Vitvi05g02256	Vitvi03g01867	Vitvi07g00732
Vitvi00g02232	Vitvi17g01735	Vitvi00g01963	Vitvi02g01587	Vitvi15g01678	Vitvi18g00664
Vitvi14g02660	Vitvi15g01136	Vitvi08g01637	Vitvi09g00142	Vitvi13g02089	Vitvi01g00603
Vitvi09g00177	Vitvi19g02311	Vitvi10g01391	Vitvi06g00553	Vitvi13g01562	Vitvi05g00221
Vitvi00g02336	Vitvi09g01552	Vitvi01g00953	Vitvi10g00110	Vitvi06g01905	Vitvi08g01718
Vitvi14g00649	Vitvi03g01404	Vitvi08g01423	Vitvi05g00509	Vitvi18g03391	Vitvi10g00469
Vitvi12g02178	Vitvi04g00859	Vitvi19g00410	Vitvi12g00555	Vitvi10g00866	Vitvi06g01375
Vitvi18g03059	Vitvi11g00764	Vitvi10g01632	Vitvi18g02401	Vitvi12g00196	Vitvi03g00488
Vitvi18g02887	Vitvi07g02430	Vitvi03g01572	Vitvi07g01764	Vitvi14g00675	Vitvi05g00271
Vitvi03g01483	Vitvi02g00526	Vitvi02g00114	Vitvi08g02182	Vitvi11g01350	Vitvi15g01681
Vitvi07g01970	Vitvi08g01634	Vitvi18g02692	Vitvi09g01752	Vitvi12g00351	Vitvi07g00164

Table A1. Cont.

A (376 Genes)	B (309 Genes)	C (340 Genes)	D (384 Genes)	E (462 Genes)	F (695 Genes)
Vitvi12g02435	Vitvi05g01938	Vitvi07g01429	Vitvi07g01475	Vitvi14g02535	Vitvi03g00445
Vitvi18g03126	Vitvi13g00716	Vitvi07g02538	Vitvi14g00465	Vitvi12g02628	Vitvi13g01337
Vitvi13g01956	Vitvi14g01647	Vitvi15g00889	Vitvi19g01788	Vitvi18g02954	Vitvi19g00198
Vitvi02g00055	Vitvi19g02128	Vitvi16g01480	Vitvi10g00751	Vitvi13g02410	Vitvi07g01644
Vitvi15g00522	Vitvi14g01646	Vitvi09g01605	Vitvi02g01442	Vitvi01g02166	Vitvi08g02386
Vitvi13g02064	Vitvi03g01773	Vitvi06g01559	Vitvi12g02254	Vitvi18g03336	Vitvi04g00470
Vitvi03g00678	Vitvi04g00407	Vitvi18g01264	Vitvi17g01613	Vitvi16g01603	Vitvi01g01236
Vitvi05g01276	Vitvi14g01642	Vitvi06g00024	Vitvi07g01856	Vitvi07g02720	Vitvi07g02029
Vitvi14g02934	Vitvi14g00301	Vitvi11g00165	Vitvi12g00632	Vitvi10g02060	Vitvi02g00286
Vitvi01g02237	Vitvi13g01307	Vitvi03g01596	Vitvi13g01888	Vitvi17g00994	Vitvi02g01022
Vitvi06g00008	Vitvi03g01877	Vitvi17g01465	Vitvi19g01825	Vitvi18g02969	Vitvi18g00628
Vitvi18g03094	Vitvi05g02089	Vitvi18g00882	Vitvi01g01181	Vitvi02g00126	Vitvi18g02780
Vitvi10g01552	Vitvi02g01003	Vitvi18g02589	Vitvi18g02495	Vitvi12g02291	Vitvi10g00559
Vitvi18g03001	Vitvi04g00831	Vitvi16g01262	Vitvi11g00431	Vitvi07g02393	Vitvi03g01431
Vitvi18g03358	Vitvi16g01886	Vitvi05g01860	Vitvi10g01825	Vitvi09g01801	Vitvi18g00189
Vitvi19g00962	Vitvi16g00160	Vitvi10g01857	Vitvi00g01122	Vitvi14g02786	Vitvi16g00504
Vitvi09g01210	Vitvi03g00924	Vitvi18g02630	Vitvi13g01425	Vitvi18g02028	Vitvi07g01552
Vitvi13g01638	Vitvi13g02605	Vitvi17g00293	Vitvi06g00380	Vitvi10g00960	Vitvi14g00065
Vitvi06g01099	Vitvi16g00122	Vitvi08g00793	Vitvi09g01951	Vitvi12g02255	Vitvi14g02458
Vitvi01g01054	Vitvi05g00963	Vitvi19g00039	Vitvi10g02187	Vitvi08g02455	Vitvi04g01801
Vitvi05g01435	Vitvi09g01569	Vitvi13g02369	Vitvi02g00697	Vitvi19g02168	Vitvi03g01232
Vitvi04g02195	Vitvi11g01231	Vitvi18g00473	Vitvi16g01169	Vitvi05g01738	Vitvi18g00131
Vitvi14g00041	Vitvi10g02128	Vitvi03g01352	Vitvi06g01324	Vitvi03g01619	Vitvi04g00524
Vitvi16g00275	Vitvi07g01867	Vitvi16g01336	Vitvi11g00010	Vitvi10g01635	Vitvi02g00433
Vitvi13g01102	Vitvi18g00143	Vitvi03g01350	Vitvi01g02137	Vitvi10g01596	Vitvi18g00510
Vitvi08g01055	Vitvi16g00118	Vitvi03g01651	Vitvi03g01857	Vitvi18g03399	Vitvi12g02200
Vitvi19g01631	Vitvi09g01792	Vitvi18g02617	Vitvi03g00427	Vitvi14g02649	Vitvi12g00025
Vitvi11g01660	Vitvi01g00066	Vitvi06g00665	Vitvi11g00081	Vitvi07g02372	Vitvi03g00439
Vitvi12g02476	Vitvi12g01264	Vitvi18g00260	Vitvi12g00290	Vitvi15g01655	Vitvi08g00820
Vitvi02g01758	Vitvi15g00078	Vitvi03g01196	Vitvi03g01412	Vitvi18g01777	Vitvi04g02049
Vitvi15g01652	Vitvi12g01917	Vitvi13g00066	Vitvi03g01679	Vitvi08g02426	Vitvi05g00170
Vitvi14g02521	Vitvi18g00107	Vitvi04g01389	Vitvi10g01774	Vitvi15g00874	Vitvi17g00885
Vitvi14g02721	Vitvi13g01873	Vitvi03g00473	Vitvi07g02071	Vitvi18g03079	Vitvi03g00023
Vitvi12g00080	Vitvi06g01599	Vitvi16g00890	Vitvi13g01085	Vitvi14g02537	Vitvi13g02292
Vitvi07g01718	Vitvi14g02584	Vitvi14g01390	Vitvi09g00966	Vitvi12g01879	Vitvi07g02588
Vitvi14g02749	Vitvi03g00925	Vitvi18g01320	Vitvi08g01205	Vitvi10g01595	Vitvi03g01729
Vitvi14g02513	Vitvi12g00644	Vitvi08g00886	Vitvi18g00609	Vitvi10g01617	Vitvi14g00398
Vitvi13g01013	Vitvi12g02475	Vitvi10g00562	Vitvi10g02191	Vitvi15g00875	Vitvi01g00821
Vitvi12g00039	Vitvi09g00409	Vitvi10g02389	Vitvi09g01584	Vitvi11g01553	Vitvi12g02599
Vitvi02g00424	Vitvi07g00301	Vitvi18g00313	Vitvi09g01983	Vitvi11g01418	Vitvi03g00338
Vitvi12g00037	Vitvi18g03314	Vitvi14g00952	Vitvi07g02112	Vitvi10g01293	Vitvi10g00621
Vitvi17g01101	Vitvi12g02458	Vitvi04g00641	Vitvi18g02404	Vitvi11g01699	Vitvi12g01841
Vitvi19g02316	Vitvi12g02318	Vitvi08g01572	Vitvi07g00063	Vitvi11g01654	Vitvi07g00337
Vitvi12g01838	Vitvi04g01638	Vitvi18g01238	Vitvi04g00884	Vitvi01g02146	Vitvi13g00070
Vitvi04g02153	Vitvi08g02056	Vitvi03g01348	Vitvi12g02657	Vitvi07g02258	Vitvi05g00402
Vitvi05g01288	Vitvi10g02215	Vitvi15g01495	Vitvi18g00366	Vitvi13g02539	Vitvi18g00691
Vitvi16g01529	Vitvi09g01770	Vitvi02g01407	Vitvi15g01204	Vitvi09g01675	Vitvi10g00442
Vitvi00g00889	Vitvi07g00899	Vitvi18g02730	Vitvi00g01940	Vitvi03g01859	Vitvi01g00264
Vitvi04g02194	Vitvi01g00739	Vitvi09g01581	Vitvi01g01836	Vitvi09g00902	Vitvi17g01318
Vitvi09g01141	Vitvi13g01945	Vitvi18g00061	Vitvi13g01969	Vitvi05g01985	Vitvi12g02147
Vitvi06g00610	Vitvi03g00702	Vitvi02g00017	Vitvi01g00566	Vitvi02g01673	Vitvi04g01799
Vitvi18g02060	Vitvi09g01181	Vitvi13g01001	Vitvi06g00351	Vitvi10g02061	Vitvi14g01637
Vitvi13g00127	Vitvi07g02109	Vitvi10g01624	Vitvi15g00754	Vitvi04g02061	Vitvi07g00542
Vitvi18g01914	Vitvi18g02455	Vitvi03g00936	Vitvi12g01832	Vitvi19g02066	Vitvi18g00268
Vitvi17g01397	Vitvi10g02170	Vitvi11g00365	Vitvi16g01779	Vitvi18g01585	Vitvi02g00052
Vitvi12g02641	Vitvi15g01687	Vitvi02g01705	Vitvi10g01795	Vitvi10g01993	Vitvi14g01341
Vitvi19g00484	Vitvi08g01293	Vitvi17g00955	Vitvi14g02455	Vitvi15g01448	Vitvi10g00399
Vitvi11g01105	Vitvi18g02628	Vitvi03g01358	Vitvi01g00680	Vitvi12g02284	Vitvi13g00143

Table A1. Cont.

A (376 Genes)	B (309 Genes)	C (340 Genes)	D (384 Genes)	E (462 Genes)	F (695 Genes)
Vitvi19g00412	Vitvi14g02408	Vitvi15g00641	Vitvi14g03087	Vitvi15g01722	Vitvi02g01446
Vitvi00g02220	Vitvi13g01874	Vitvi11g00838	Vitvi10g02081	Vitvi14g02737	Vitvi05g00377
Vitvi01g00796	Vitvi00g01102	Vitvi08g01348	Vitvi07g01658	Vitvi15g01379	Vitvi19g02064
Vitvi05g01903	Vitvi16g01884	Vitvi06g01921	Vitvi16g00879	Vitvi02g01590	Vitvi05g01901
Vitvi04g02197	Vitvi07g03001	Vitvi04g01635	Vitvi06g01638	Vitvi09g01918	Vitvi04g01653
Vitvi10g00535	Vitvi09g01791	Vitvi01g00864	Vitvi13g01861	Vitvi09g01820	Vitvi19g00682
Vitvi12g00002	Vitvi07g02477	Vitvi04g00735	Vitvi18g01168	Vitvi18g03021	Vitvi06g01459
Vitvi18g02857	Vitvi01g02000	Vitvi10g01715	Vitvi05g00126	Vitvi19g01041	Vitvi10g01756
Vitvi14g01402	Vitvi12g02179	Vitvi17g01520	Vitvi18g02661	Vitvi09g00918	Vitvi05g02177
Vitvi18g01376	Vitvi14g00775	Vitvi08g02121	Vitvi18g02648	Vitvi18g03389	Vitvi13g02075
Vitvi12g01911	Vitvi06g01944	Vitvi14g02558	Vitvi07g01759	Vitvi15g01749	Vitvi03g00397
Vitvi16g00022	Vitvi14g01645	Vitvi10g01029	Vitvi08g02381	Vitvi09g00808	Vitvi05g00864
Vitvi05g01469	Vitvi07g02368	Vitvi12g00251	Vitvi04g00801	Vitvi14g02675	Vitvi15g00396
Vitvi10g01651	Vitvi05g00604	Vitvi08g01342	Vitvi05g01259	Vitvi04g02060	Vitvi07g00176
Vitvi12g02125	Vitvi16g00129	Vitvi16g01175	Vitvi19g01727	Vitvi10g01823	Vitvi03g00443
Vitvi09g01371	Vitvi05g00381	Vitvi15g00921	Vitvi05g00861	Vitvi02g01784	Vitvi15g01021
Vitvi05g00523	Vitvi03g01531	Vitvi19g00041	Vitvi12g00148	Vitvi09g00884	Vitvi17g00098
Vitvi10g00519	Vitvi17g01395	Vitvi16g01979	Vitvi05g01828	Vitvi11g01360	Vitvi15g00915
Vitvi13g02425	Vitvi03g01525	Vitvi19g00397	Vitvi15g00929	Vitvi18g03317	Vitvi02g01358
Vitvi19g01061	Vitvi14g01805	Vitvi13g02005	Vitvi14g00243	Vitvi17g00593	Vitvi13g00076
Vitvi05g02199	Vitvi12g02639	Vitvi01g00477	Vitvi09g00241	Vitvi15g01717	Vitvi04g00241
Vitvi04g01895	Vitvi13g01684	Vitvi09g01398	Vitvi07g02228	Vitvi18g03345	Vitvi09g01409
Vitvi01g01886	Vitvi02g00521	Vitvi13g02009	Vitvi13g01871	Vitvi09g01956	Vitvi14g02990
Vitvi01g02020	Vitvi11g00634	Vitvi11g01681	Vitvi19g02118	Vitvi14g02545	Vitvi04g02087
Vitvi01g00815	Vitvi03g00411	Vitvi15g00537	Vitvi13g02023	Vitvi14g00220	Vitvi11g01532
Vitvi03g01571	Vitvi11g01634	Vitvi03g01597	Vitvi01g01437	Vitvi00g02009	Vitvi05g00046
Vitvi18g03182	Vitvi16g01123	Vitvi05g00360	Vitvi08g02368	Vitvi18g01839	Vitvi11g00727
Vitvi12g02259	Vitvi18g02993	Vitvi08g01789	Vitvi08g02325	Vitvi18g02942	Vitvi11g01428
Vitvi05g01453	Vitvi18g00204	Vitvi07g01734	Vitvi18g01637	Vitvi15g01331	Vitvi09g00995
Vitvi17g01476	Vitvi19g00479	Vitvi03g01361	Vitvi04g02308	Vitvi16g01651	Vitvi18g03254
Vitvi14g02522	Vitvi03g01522	Vitvi18g02075	Vitvi16g01952	Vitvi14g02873	Vitvi03g01430
Vitvi11g01471	Vitvi16g01800	Vitvi13g01744	Vitvi08g00108	Vitvi15g01343	Vitvi13g00405
Vitvi02g00811	Vitvi13g01876	Vitvi18g02616	Vitvi13g02043	Vitvi11g01497	Vitvi03g01428
Vitvi12g02231	Vitvi03g01742	Vitvi07g01847	Vitvi01g00892	Vitvi00g01834	Vitvi04g01795
Vitvi19g00052	Vitvi11g00950	Vitvi02g00022	Vitvi15g01647	Vitvi15g01739	Vitvi08g01089
Vitvi19g01863	Vitvi03g00699	Vitvi08g02126	Vitvi10g02083	Vitvi18g02701	Vitvi08g01276
Vitvi18g00623	Vitvi18g00816	Vitvi05g00478	Vitvi09g00021	Vitvi18g03024	Vitvi18g02754
Vitvi19g02236	Vitvi14g01318	Vitvi12g02434	Vitvi09g01603	Vitvi09g00916	Vitvi18g02399
Vitvi18g01763	Vitvi12g02213	Vitvi04g00060	Vitvi11g01266	Vitvi06g01870	Vitvi08g01602
Vitvi07g02711	Vitvi12g01172	Vitvi10g01628	Vitvi01g01885	Vitvi18g03350	Vitvi14g01865
Vitvi05g01156	Vitvi13g02592	Vitvi04g02239	Vitvi14g02477	Vitvi13g01254	Vitvi07g02433
Vitvi15g01425	Vitvi10g01699	Vitvi04g01160	Vitvi10g01017	Vitvi17g00009	Vitvi16g01352
Vitvi06g00547	Vitvi14g01907	Vitvi01g00612	Vitvi10g02214	Vitvi07g02673	Vitvi01g01654
Vitvi13g02459	Vitvi07g02413	Vitvi10g01023	Vitvi17g01427	Vitvi09g02096	Vitvi04g00527
Vitvi03g00574	Vitvi07g01837	Vitvi01g01808	Vitvi04g01264	Vitvi10g01392	Vitvi17g00565
Vitvi17g00224	Vitvi12g02523	Vitvi01g00656	Vitvi09g00717	Vitvi03g01737	Vitvi11g00183
Vitvi10g01930	Vitvi03g01819	Vitvi03g01364	Vitvi09g00472	Vitvi03g01674	Vitvi01g00424
Vitvi06g00672	Vitvi03g01530	Vitvi10g01623	Vitvi09g01490	Vitvi09g01526	Vitvi07g00807
Vitvi05g02208	Vitvi10g01455	Vitvi08g00868	Vitvi09g00621	Vitvi12g02762	Vitvi14g02811
Vitvi16g00715	Vitvi12g02317	Vitvi08g01024	Vitvi06g01574	Vitvi17g01539	Vitvi00g01020
Vitvi19g02392	Vitvi19g01636	Vitvi01g00608	Vitvi08g02282	Vitvi16g02154	Vitvi09g00007
Vitvi08g01846	Vitvi03g01528	Vitvi03g00144	Vitvi15g01641	Vitvi18g02899	Vitvi10g00276
Vitvi00g01239	Vitvi11g01442	Vitvi15g01035	Vitvi17g00556	Vitvi12g02257	Vitvi01g01038
Vitvi19g01371	Vitvi12g02324	Vitvi17g00292	Vitvi11g01366	Vitvi18g02901	Vitvi11g00317
Vitvi05g00109	Vitvi19g01525	Vitvi18g01098	Vitvi09g01851	Vitvi10g02044	Vitvi04g00106
Vitvi18g01919	Vitvi12g01431	Vitvi07g03142	Vitvi07g01728	Vitvi12g02605	Vitvi12g02495
Vitvi16g00900	Vitvi18g01849	Vitvi19g00141	Vitvi18g00746	Vitvi18g03025	Vitvi05g00486
Vitvi18g00153	Vitvi11g01437	Vitvi19g02057	Vitvi14g02599	Vitvi03g01785	Vitvi15g00906

Table A1. Cont.

A (376 Genes)	B (309 Genes)	C (340 Genes)	D (384 Genes)	E (462 Genes)	F (695 Genes)
Vitvi00g01276	Vitvi05g01944	Vitvi18g00274	Vitvi18g02534	Vitvi09g00886	Vitvi00g01061
Vitvi10g01910	Vitvi07g02404	Vitvi07g01737	Vitvi16g01132	Vitvi15g01356	Vitvi05g01786
Vitvi03g01591	Vitvi12g02634	Vitvi07g03112	Vitvi05g02255	Vitvi03g00933	Vitvi19g00153
Vitvi05g01419	Vitvi03g01535	Vitvi16g01176	Vitvi13g02139	Vitvi14g01946	Vitvi18g00435
Vitvi18g03095	Vitvi04g02252	Vitvi17g00046	Vitvi07g02858	Vitvi09g02095	Vitvi07g02265
Vitvi09g01914	Vitvi12g01323	Vitvi09g00193	Vitvi17g01357	Vitvi18g02896	Vitvi08g00014
Vitvi19g01832	Vitvi05g02253	Vitvi17g00977	Vitvi10g02241	Vitvi06g00266	Vitvi07g02240
Vitvi08g01972	Vitvi08g01235	Vitvi04g00680	Vitvi09g01982	Vitvi13g02143	Vitvi08g00030
Vitvi12g02701	Vitvi03g01482	Vitvi07g01773	Vitvi18g02838	Vitvi18g03083	Vitvi04g00636
Vitvi02g01355	Vitvi08g02266	Vitvi13g00669	Vitvi19g01896	Vitvi18g02902	Vitvi12g02138
Vitvi05g01617	Vitvi11g00001	Vitvi11g00811	Vitvi16g00971	Vitvi08g02464	Vitvi05g01571
Vitvi09g02007	Vitvi05g01945	Vitvi10g00605	Vitvi02g01325	Vitvi15g01389	Vitvi16g01164
Vitvi09g01790	Vitvi11g01576	Vitvi08g00970	Vitvi00g00989	Vitvi10g02105	Vitvi13g00591
Vitvi09g01912	Vitvi16g00787	Vitvi13g01932	Vitvi04g00696	Vitvi07g02373	Vitvi05g01350
Vitvi16g01699	Vitvi18g00878	Vitvi16g01418	Vitvi18g02591	Vitvi10g01195	Vitvi01g00673
Vitvi18g01959	Vitvi04g00432	Vitvi05g01269	Vitvi04g00136	Vitvi11g01357	Vitvi08g02163
Vitvi18g01877	Vitvi03g01486	Vitvi03g01363	Vitvi14g02655	Vitvi15g01665	Vitvi19g01902
Vitvi02g01354	Vitvi16g00349	Vitvi03g01292	Vitvi19g01948	Vitvi18g03038	Vitvi19g00515
Vitvi12g00452	Vitvi08g00267	Vitvi13g00012	Vitvi08g00155	Vitvi18g02949	Vitvi04g01095
Vitvi03g01540	Vitvi18g00444	Vitvi02g00327	Vitvi13g01267	Vitvi07g02378	Vitvi01g01304
Vitvi15g01705	Vitvi06g01060	Vitvi04g00289	Vitvi18g00807	Vitvi14g00223	Vitvi08g01767
Vitvi11g00882	Vitvi19g02009	Vitvi04g02238	Vitvi02g01744	Vitvi04g02018	Vitvi01g02158
Vitvi18g02198	Vitvi04g02310	Vitvi07g02990	Vitvi08g01503	Vitvi00g02357	Vitvi13g01107
Vitvi19g02286	Vitvi05g01200	Vitvi03g01872	Vitvi16g01325	Vitvi15g01323	Vitvi14g01344
Vitvi05g02141	Vitvi15g00675	Vitvi05g00067	Vitvi19g01601	Vitvi10g01519	Vitvi09g00599
Vitvi19g01217		Vitvi18g00687	Vitvi15g01642	Vitvi19g01821	Vitvi07g01454
Vitvi14g01938		Vitvi15g00753	Vitvi03g00047	Vitvi15g00494	Vitvi04g02313
Vitvi05g00485		Vitvi05g00802	Vitvi13g01245	Vitvi18g02905	Vitvi09g00223
Vitvi10g01431		Vitvi04g01934	Vitvi10g00439	Vitvi01g02168	Vitvi17g01050
Vitvi14g00025		Vitvi17g01389	Vitvi02g01363	Vitvi05g02073	Vitvi01g00292
Vitvi12g02153		Vitvi04g00722	Vitvi14g00401	Vitvi18g03341	Vitvi04g01097
Vitvi17g00306		Vitvi08g01190	Vitvi04g02221	Vitvi05g02103	Vitvi14g00185
Vitvi06g01765		Vitvi07g02987	Vitvi05g02050	Vitvi14g02536	Vitvi10g00946
Vitvi06g01334		Vitvi07g01240	Vitvi19g02049	Vitvi18g02936	Vitvi19g00164
Vitvi07g01714		Vitvi01g00638	Vitvi09g01980	Vitvi18g02947	Vitvi12g00026
Vitvi11g00013		Vitvi05g00637	Vitvi19g02025	Vitvi10g01989	Vitvi13g00278
Vitvi10g01941		Vitvi16g01078	Vitvi01g02124	Vitvi10g01201	Vitvi02g00938
Vitvi18g03362		Vitvi02g00532	Vitvi14g02868	Vitvi15g01677	Vitvi07g01596
Vitvi05g02085		Vitvi13g00375	Vitvi14g02781	Vitvi18g02953	Vitvi02g00374
Vitvi14g00577		Vitvi14g03042	Vitvi09g01742	Vitvi16g01764	Vitvi08g00808
Vitvi14g02692		Vitvi10g02177	Vitvi12g02737	Vitvi18g02944	Vitvi08g01126
Vitvi05g01153		Vitvi06g01830	Vitvi14g02497	Vitvi04g00352	Vitvi02g00223
Vitvi14g00707		Vitvi07g00400	Vitvi06g01711	Vitvi15g00323	Vitvi03g00378
Vitvi18g01962		Vitvi18g01735	Vitvi14g03007	Vitvi16g01622	Vitvi19g00029
Vitvi04g00433		Vitvi19g00735	Vitvi06g00359	Vitvi16g01738	Vitvi09g00582
Vitvi17g00309		Vitvi16g00071	Vitvi14g00997	Vitvi16g00859	Vitvi17g01593
Vitvi12g01861		Vitvi09g01122	Vitvi07g00822	Vitvi07g00478	Vitvi02g00228
Vitvi01g00088		Vitvi12g00721	Vitvi12g02258	Vitvi09g01142	Vitvi07g01354
Vitvi16g01278		Vitvi07g02989	Vitvi15g01560	Vitvi18g03061	Vitvi11g01602
Vitvi13g02470		Vitvi09g00185	Vitvi16g01312	Vitvi19g01083	Vitvi14g02009
Vitvi12g01908		Vitvi09g01954	Vitvi04g02207	Vitvi13g02439	Vitvi06g00329
Vitvi19g01820		Vitvi18g01253	Vitvi05g01611	Vitvi10g01829	Vitvi10g00209
Vitvi03g00504		Vitvi07g02573	Vitvi13g02489	Vitvi09g00682	Vitvi06g00785
Vitvi16g02028		Vitvi11g00360	Vitvi13g00388	Vitvi02g01280	Vitvi07g02634
Vitvi05g02155		Vitvi11g00417	Vitvi12g00648	Vitvi16g01760	Vitvi01g00309
Vitvi13g00940		Vitvi11g00089	Vitvi05g01451	Vitvi18g03067	Vitvi10g01641
Vitvi18g01716			Vitvi08g01991	Vitvi00g02238	Vitvi02g00265
Vitvi05g01923			Vitvi05g01768	Vitvi19g01836	Vitvi18g00149

Table A1. Cont.

A (376 Genes)	B (309 Genes)	C (340 Genes)	D (384 Genes)	E (462 Genes)	F (695 Genes)
Vitvi13g02026			Vitvi05g02093	Vitvi14g02554	Vitvi03g01337
Vitvi18g02649			Vitvi05g01370	Vitvi16g00391	Vitvi07g01078
Vitvi08g01110			Vitvi10g02035	Vitvi17g01046	Vitvi07g03014
Vitvi07g01045			Vitvi08g01938	Vitvi00g01769	Vitvi13g01066
Vitvi17g01286			Vitvi05g00411	Vitvi18g03022	Vitvi04g00846
Vitvi07g02077			Vitvi18g02656	Vitvi19g01929	Vitvi15g01575
Vitvi19g01850			Vitvi03g00953	Vitvi02g01764	Vitvi09g01204
Vitvi04g01836			Vitvi14g00296	Vitvi05g02036	Vitvi06g00709
Vitvi19g01824			Vitvi05g02147	Vitvi15g01330	Vitvi02g00409
Vitvi11g01181			Vitvi12g00549	Vitvi17g01673	Vitvi08g01470
Vitvi05g00905			Vitvi05g02144	Vitvi18g02703	Vitvi07g02595
Vitvi18g03217			Vitvi09g00475	Vitvi05g00152	Vitvi12g00414
Vitvi18g00154			Vitvi06g00078	Vitvi10g01620	Vitvi01g00246
Vitvi13g02473			Vitvi05g01530	Vitvi15g00918	Vitvi09g02017
Vitvi07g01719			Vitvi15g01450	Vitvi09g00914	Vitvi17g01122
Vitvi09g00356			Vitvi13g00948	Vitvi19g01950	Vitvi13g01556
Vitvi09g00867			Vitvi10g01121	Vitvi12g02763	Vitvi02g00719
Vitvi01g00873			Vitvi04g02214	Vitvi12g02189	Vitvi19g00071
Vitvi13g00037			Vitvi13g00458	Vitvi18g02698	Vitvi13g01778
Vitvi01g01949			Vitvi10g00478	Vitvi13g01676	Vitvi08g02168
Vitvi18g00470			Vitvi16g00515	Vitvi16g01461	Vitvi11g00022
Vitvi12g02726			Vitvi14g01053	Vitvi07g02665	Vitvi08g02184
Vitvi14g02004			Vitvi06g01233	Vitvi12g02730	Vitvi07g01329
Vitvi18g00191			Vitvi03g01336	Vitvi13g02423	Vitvi11g00336
Vitvi13g02028			Vitvi18g00604	Vitvi08g02081	Vitvi01g00637
Vitvi13g00425			Vitvi02g00181	Vitvi18g02873	Vitvi07g01816
Vitvi15g01710			Vitvi08g02221	Vitvi01g02134	Vitvi01g02263
Vitvi19g00101			Vitvi13g02241	Vitvi09g00809	Vitvi07g01273
Vitvi11g01270			Vitvi14g02977	Vitvi18g03065	Vitvi12g00560
Vitvi16g01701			Vitvi16g01491	Vitvi10g01599	Vitvi04g01261
Vitvi00g02329			Vitvi01g02178	Vitvi19g02229	Vitvi17g01625
Vitvi05g00930			Vitvi15g00570	Vitvi16g01465	Vitvi07g02969
Vitvi01g02105			Vitvi01g00546	Vitvi13g02583	Vitvi18g00181
Vitvi13g00474			Vitvi04g00774	Vitvi16g00321	Vitvi10g00687
			Vitvi16g01955	Vitvi10g01598	Vitvi10g01605
			Vitvi03g01098	Vitvi18g03356	Vitvi16g01103
			Vitvi08g01369	Vitvi08g02159	Vitvi04g00264
			Vitvi18g01533	Vitvi12g01701	Vitvi15g00998
			Vitvi17g01373	Vitvi18g03027	Vitvi12g00221
			Vitvi09g01553	Vitvi18g03351	Vitvi06g00494
			Vitvi08g02046	Vitvi15g01253	Vitvi12g00086
			Vitvi10g01095	Vitvi03g01682	Vitvi01g02030
				Vitvi15g00308	Vitvi12g00542
				Vitvi03g00407	Vitvi14g01685
				Vitvi16g01824	Vitvi09g00568
				Vitvi07g02360	Vitvi06g00518
				Vitvi05g02210	Vitvi08g01724
				Vitvi14g02552	Vitvi05g00539
				Vitvi15g01704	Vitvi05g02190
				Vitvi17g01464	Vitvi06g01057
				Vitvi07g02357	Vitvi08g02261
				Vitvi07g02315	Vitvi05g00736
				Vitvi18g03039	Vitvi07g00015
				Vitvi03g01732	Vitvi04g02297
				Vitvi14g02532	Vitvi10g01540
				Vitvi04g00723	Vitvi02g01778
				Vitvi08g02255	Vitvi05g01833
				Vitvi16g01459	Vitvi08g02225

Table A1. Cont.

A (376 Genes)	B (309 Genes)	C (340 Genes)	D (384 Genes)	E (462 Genes)	F (695 Genes)
				Vitvi18g02668	Vitvi17g01474
				Vitvi08g00728	Vitvi05g01855
				Vitvi16g02161	Vitvi08g01011
				Vitvi10g01313	Vitvi18g00283
				Vitvi04g02215	Vitvi04g00047
				Vitvi15g01419	Vitvi16g01830
				Vitvi18g03033	Vitvi08g01406
				Vitvi01g02143	Vitvi10g01103
				Vitvi02g00809	Vitvi05g01113
				Vitvi14g02534	Vitvi09g01273
				Vitvi18g02895	Vitvi19g00113
				Vitvi12g02425	Vitvi04g02296
				Vitvi09g01957	Vitvi06g00074
				Vitvi03g01446	Vitvi06g00202
				Vitvi09g01778	Vitvi08g01839
				Vitvi01g02311	Vitvi10g00612
				Vitvi18g02723	Vitvi13g01068
				Vitvi12g02662	Vitvi07g01766
				Vitvi10g01824	Vitvi19g01917
				Vitvi17g00458	Vitvi06g01709
				Vitvi14g02787	Vitvi10g00711
				Vitvi10g02008	Vitvi05g00128
				Vitvi09g02051	Vitvi14g01721
				Vitvi10g00504	Vitvi18g00694
				Vitvi03g01359	Vitvi09g01519
				Vitvi09g01757	Vitvi05g00337
				Vitvi15g01360	Vitvi05g00218
				Vitvi07g00957	Vitvi07g01363
				Vitvi05g01982	Vitvi16g00553
				Vitvi17g01630	Vitvi10g00465
				Vitvi06g01720	Vitvi17g00892
				Vitvi04g02193	Vitvi04g00252
				Vitvi18g03174	Vitvi14g02461
				Vitvi03g01640	Vitvi10g00694
				Vitvi10g02052	Vitvi10g01250
				Vitvi03g01663	Vitvi04g01296
				Vitvi16g01608	Vitvi17g00757
				Vitvi09g01971	Vitvi14g01305
				Vitvi15g01319	Vitvi16g01217
				Vitvi14g00676	Vitvi01g00363
				Vitvi11g00982	Vitvi08g01040
				Vitvi12g01849	Vitvi16g02078
				Vitvi04g00349	Vitvi07g01325
				Vitvi12g02182	Vitvi18g02813
				Vitvi18g03403	Vitvi10g00880
				Vitvi00g01835	Vitvi11g00284
				Vitvi18g02104	Vitvi07g00444
				Vitvi04g00874	Vitvi04g00090
				Vitvi00g01893	Vitvi10g00266
				Vitvi19g02363	Vitvi02g01644
				Vitvi12g00509	Vitvi04g01802
				Vitvi09g01626	Vitvi00g00894
				Vitvi12g01154	Vitvi08g01550
				Vitvi10g01964	Vitvi06g00548
				Vitvi14g03088	Vitvi14g02462
				Vitvi16g00442	Vitvi13g00994
				Vitvi03g01714	Vitvi16g00518
				Vitvi09g02085	Vitvi09g00355

Table A1. Cont.

A (376 Genes)	B (309 Genes)	C (340 Genes)	D (384 Genes)	E (462 Genes)	F (695 Genes)
				Vitvi01g02312	Vitvi08g01013
				Vitvi12g00920	Vitvi19g00285
				Vitvi01g02156	Vitvi10g00705
				Vitvi03g01793	Vitvi17g01275
				Vitvi06g00465	Vitvi06g00569
				Vitvi18g01217	Vitvi06g00299
				Vitvi14g00902	Vitvi14g02457
				Vitvi07g02753	Vitvi07g00105
				Vitvi14g00152	Vitvi14g01859
				Vitvi06g01635	Vitvi06g00936
				Vitvi17g00918	Vitvi17g00034
				Vitvi14g01524	Vitvi16g01126
				Vitvi03g00579	Vitvi01g01583
				Vitvi17g00384	Vitvi06g00774
				Vitvi16g00921	Vitvi13g00865
				Vitvi19g02276	Vitvi19g00276
				Vitvi02g00499	Vitvi02g00499
				Vitvi17g00030	Vitvi09g00187
				Vitvi15g01146	Vitvi15g00684
				Vitvi18g00708	Vitvi18g02420
				Vitvi18g02420	Vitvi02g01314
				Vitvi12g00771	Vitvi12g00771
				Vitvi04g01664	Vitvi04g01664
				Vitvi11g00231	Vitvi11g00231
				Vitvi01g00941	Vitvi01g00941
				Vitvi06g00169	Vitvi06g00169
				Vitvi04g01100	Vitvi04g01100
				Vitvi11g00413	Vitvi11g00413
				Vitvi09g00647	Vitvi09g00647
				Vitvi05g00841	Vitvi05g00841
				Vitvi06g00757	Vitvi06g00757
				Vitvi03g00104	Vitvi03g00104
				Vitvi09g00166	Vitvi09g00166
				Vitvi04g01883	Vitvi04g01883
				Vitvi05g01848	Vitvi05g01848
				Vitvi03g01328	Vitvi03g01328
				Vitvi12g00729	Vitvi12g00729
				Vitvi10g00011	Vitvi10g00011
				Vitvi19g02045	Vitvi19g02045
				Vitvi11g00459	Vitvi11g00459
				Vitvi13g00270	Vitvi13g00270
				Vitvi05g02077	Vitvi05g02077
				Vitvi15g00989	Vitvi15g00989
				Vitvi14g00063	Vitvi14g00063
				Vitvi06g01621	Vitvi06g01621

Table A1. Cont.

A (376 Genes)	B (309 Genes)	C (340 Genes)	D (384 Genes)	E (462 Genes)	F (695 Genes)
					Vitvi17g00631
					Vitvi05g02181
					Vitvi08g00145
					Vitvi10g01086
					Vitvi02g00025
					Vitvi04g01529
					Vitvi18g01170
					Vitvi01g00078
					Vitvi00g01106
					Vitvi01g00648
					Vitvi18g01237
					Vitvi19g00572
					Vitvi19g00190
					Vitvi12g00383
					Vitvi14g01796
					Vitvi06g01673
					Vitvi10g00470
					Vitvi14g01894
					Vitvi07g01333
					Vitvi16g00024
					Vitvi04g00091
					Vitvi02g00482
					Vitvi18g00145
					Vitvi03g00230
					Vitvi19g00470
					Vitvi05g00575
					Vitvi09g00772
					Vitvi17g00578
					Vitvi01g00825
					Vitvi14g01984
					Vitvi19g00012
					Vitvi01g00150
					Vitvi01g00903
					Vitvi18g01173
					Vitvi05g00513
					Vitvi02g01274
					Vitvi07g00457
					Vitvi18g02501
					Vitvi07g02191
					Vitvi05g00770
					Vitvi02g01779
					Vitvi05g00535
					Vitvi03g01432
					Vitvi05g00628
					Vitvi15g00740
					Vitvi05g01048
					Vitvi07g02172
					Vitvi08g01119
					Vitvi19g00182
					Vitvi07g02971
					Vitvi08g00217
					Vitvi01g01826
					Vitvi10g02169
					Vitvi11g01241
					Vitvi15g00691
					Vitvi16g01135
					Vitvi05g00538
					Vitvi13g01253

Table A1. Cont.

A (376 Genes)	B (309 Genes)	C (340 Genes)	D (384 Genes)	E (462 Genes)	F (695 Genes)
					Vitvi13g02017
					Vitvi09g00045
					Vitvi15g00886
					Vitvi12g00714
					Vitvi18g00055
					Vitvi12g00426
					Vitvi02g01192
					Vitvi04g01159
					Vitvi08g01408
					Vitvi16g00183
					Vitvi18g01661
					Vitvi03g01805
					Vitvi00g00951
					Vitvi10g01471
					Vitvi02g00454
					Vitvi09g00165
					Vitvi04g00317
					Vitvi07g00701
					Vitvi08g00798
					Vitvi07g00048
					Vitvi05g00012
					Vitvi06g00944
					Vitvi13g00274
					Vitvi18g02052
					Vitvi04g02184
					Vitvi14g00475
					Vitvi14g02562
					Vitvi12g00486
					Vitvi10g00113
					Vitvi08g02411
					Vitvi18g00795
					Vitvi04g01792
					Vitvi17g00634
					Vitvi14g00495
					Vitvi01g01173
					Vitvi04g00210
					Vitvi02g01313
					Vitvi11g00411
					Vitvi10g02166
					Vitvi00g01333
					Vitvi07g02170
					Vitvi10g01360
					Vitvi17g00415
					Vitvi04g01800
					Vitvi18g02796
					Vitvi02g00018
					Vitvi00g00816
					Vitvi17g00071
					Vitvi11g00249
					Vitvi14g01730
					Vitvi05g01117
					Vitvi02g01211
					Vitvi17g00661
					Vitvi00g01309
					Vitvi02g00563
					Vitvi06g01119
					Vitvi06g01000
					Vitvi12g00144

Table A1. Cont.

A (376 Genes)	B (309 Genes)	C (340 Genes)	D (384 Genes)	E (462 Genes)	F (695 Genes)
					<i>Vitvi18g00719</i>
					<i>Vitvi01g01476</i>
					<i>Vitvi17g01025</i>
					<i>Vitvi08g01841</i>
					<i>Vitvi16g01306</i>
					<i>Vitvi18g01088</i>
					<i>Vitvi06g00625</i>
					<i>Vitvi16g00184</i>
					<i>Vitvi13g02507</i>
					<i>Vitvi11g00278</i>
					<i>Vitvi09g00198</i>
					<i>Vitvi06g00943</i>
					<i>Vitvi10g01422</i>
					<i>Vitvi10g01075</i>
					<i>Vitvi14g00289</i>
					<i>Vitvi01g00296</i>
					<i>Vitvi06g00538</i>
					<i>Vitvi16g01014</i>
					<i>Vitvi08g02186</i>
					<i>Vitvi06g01113</i>
					<i>Vitvi07g03100</i>
					<i>Vitvi14g00396</i>
					<i>Vitvi04g00184</i>
					<i>Vitvi14g01877</i>
					<i>Vitvi19g00652</i>
					<i>Vitvi07g01410</i>
					<i>Vitvi12g02143</i>
					<i>Vitvi04g00397</i>
					<i>Vitvi03g00376</i>
					<i>Vitvi08g01835</i>
					<i>Vitvi14g02566</i>
					<i>Vitvi03g00717</i>
					<i>Vitvi18g01448</i>
					<i>Vitvi17g00171</i>
					<i>Vitvi01g01459</i>
					<i>Vitvi10g01318</i>
					<i>Vitvi04g00962</i>
					<i>Vitvi05g00325</i>
					<i>Vitvi10g01456</i>
					<i>Vitvi13g02024</i>
					<i>Vitvi07g00581</i>
					<i>Vitvi02g00194</i>
					<i>Vitvi13g01743</i>
					<i>Vitvi18g00888</i>
					<i>Vitvi12g00576</i>
					<i>Vitvi02g01005</i>
					<i>Vitvi03g00182</i>
					<i>Vitvi16g00928</i>
					<i>Vitvi17g00114</i>
					<i>Vitvi12g00755</i>
					<i>Vitvi14g01470</i>
					<i>Vitvi14g00233</i>
					<i>Vitvi09g00997</i>
					<i>Vitvi18g01172</i>
					<i>Vitvi08g01616</i>
					<i>Vitvi09g00629</i>
					<i>Vitvi06g00506</i>
					<i>Vitvi08g01891</i>

Table A1. Cont.

A (376 Genes)	B (309 Genes)	C (340 Genes)	D (384 Genes)	E (462 Genes)	F (695 Genes)
					Vitvi14g01858
					Vitvi12g00681
					Vitvi10g00702
					Vitvi07g02242
					Vitvi08g01143

References

- Chaves, M.M.; Zarrouk, O.; Francisco, R.; Costa, J.M.; Santos, T.; Regalado, A.P.; Rodrigues, M.L.; Lopes, C.M. Grapevine under deficit irrigation: Hints from physiological and molecular data. *Ann. Bot.* **2010**, *105*, 661–676. [CrossRef] [PubMed]
- Pou, A.; Medrano, H.; Tomàs, M.; Martorell, S.; Ribas-Carbó, M.; Flexas, J. Anisohydric behaviour in grapevines results in better performance under moderate water stress and recovery than isohydric behaviour. *Plant Soil* **2012**, *359*, 335–349. [CrossRef]
- Hochberg, U.; Degu, A.; Fait, A.; Rachmilevitch, S. Near isohydric grapevine cultivar displays higher photosynthetic efficiency and photorespiration rates under drought stress as compared with near anisohydric grapevine cultivar. *Physiol. Plant.* **2013**, *147*, 443–452. [CrossRef]
- Martínez-Vilalta, J.; Garcia-Forner, N. Water potential regulation, stomatal behaviour and hydraulic transport under drought: Deconstructing the iso/anisohydric concept. *Plant Cell Environ.* **2017**, *40*, 962–976. [CrossRef]
- Schultz, H.R. Differences in hydraulic architecture account for near-isohydric and anisohydric behaviour of two field-grown *Vitis vinifera* L. cultivars during drought. *Plant Cell Environ.* **2003**, *26*, 1393–1405. [CrossRef]
- Soar, C.J.; Speirs, J.; Maffei, S.M.; Penrose, A.B.; McCarthy, M.G.; Loveys, B.R. Grape vine varieties Shiraz and Grenache differ in their stomatal response to VPD: Apparent links with ABA physiology and gene expression in leaf tissue. *Aust. J. Grape Wine Res.* **2006**, *12*, 2–12. [CrossRef]
- Tombesi, S.; Nardini, A.; Farinelli, D.; Palliotti, A. Relationships between stomatal behavior, xylem vulnerability to cavitation and leaf water relations in two cultivars of *Vitis vinifera*. *Physiol. Plant.* **2014**, *152*, 453–464. [CrossRef]
- Lavoie-Lamoureux, A.; Sacco, D.; Risso, P.-A.; Lovisolo, C. Factors influencing stomatal conductance in response to water availability in grapevine: A meta-analysis. *Physiol. Plant.* **2017**, *159*, 468–482. [CrossRef]
- Serrano, A.S.; Martínez-Gascueña, J.; Chacón-Vozmediano, J.L. Variability in water use behavior during drought of different grapevine varieties: Assessment of their regulation of water status and stomatal control. *Agric. Water Manag.* **2024**, *291*, 108642. [CrossRef]
- Rogiers, S.Y.; Greer, D.H.; Hatfield, J.M.; Hutton, R.J.; Clarke, S.J.; Hutchinson, P.A.; Somers, A. Stomatal response of an anisohydric grapevine cultivar to evaporative demand, available soil moisture and abscisic acid. *Tree Physiol.* **2012**, *32*, 249–261. [CrossRef]
- Garcia-Forner, N.; Biel, C.; Savé, R.; Martínez-Vilalta, J. Isohydric species are not necessarily more carbon limited than anisohydric species during drought. Meinzer, F. editor. *Tree Physiol.* **2017**, *37*, 441–455. [CrossRef] [PubMed]
- Yi, K.; Dragoni, D.; Phillips, R.P.; Roman, D.T.; Novick, K.A. Dynamics of stem water uptake among isohydric and anisohydric species experiencing a severe drought. *Tree Physiol.* **2017**, *37*, 1379–1392. [CrossRef]
- McDowell, N.; Pockman, W.T.; Allen, C.D.; Breshears, D.D.; Cobb, N.; Kolb, T.; Plaut, J.; Sperry, J.; West, A.; Williams, D.G.; et al. Mechanisms of plant survival and mortality during drought: Why do some plants survive while others succumb to drought? *New Phytol.* **2008**, *178*, 719–739. [CrossRef] [PubMed]
- Dayer, S.; Scharwies, J.D.; Ramesh, S.A.; Sullivan, W.; Doerflinger, F.C.; Pagay, V.; Tyerman, S.D. Comparing Hydraulics Between Two Grapevine Cultivars Reveals Differences in Stomatal Regulation Under Water Stress and Exogenous ABA Applications. *Front Plant Sci.* **2020**, *11*, 705. [CrossRef] [PubMed]
- Santo, S.D.; Palliotti, A.; Zenoni, S.; Tornielli, G.B.; Fasoli, M.; Paci, P.; Tombesi, S.; Frioni, T.; Silvestroni, O.; Bellincontro, A.; et al. Distinct transcriptome responses to water limitation in isohydric and anisohydric grapevine cultivars. *BMC Genom.* **2016**, *17*, 815. [CrossRef]
- Villalobos-González, L.; Muñoz-Araya, M.; Franck, N.; Pastenes, C. Controversies in Midday Water Potential Regulation and Stomatal Behavior Might Result from the Environment, Genotype, and/or Rootstock: Evidence from Carménère and Syrah Grapevine Varieties. *Front. Plant Sci.* **2019**, *10*, 1522. [CrossRef]
- Fu, X.; Meinzer, F.C. Metrics and proxies for stringency of regulation of plant water status (iso/anisohydry): A global data set reveals coordination and trade-offs among water transport traits. *Tree Physiol.* **2019**, *39*, 122–134. [CrossRef]
- Konecny, T.; Nikoghosyan, M.; Binder, H. Machine learning extracts marks of thiamine's role in cold acclimation in the transcriptome of *Vitis vinifera*. *Front. Plant Sci.* **2023**, *14*, 1303542. [CrossRef]
- Tusher, V.G.; Tibshirani, R.; Chu, G. Significance analysis of microarrays applied to the ionizing radiation response. *Proc. Natl. Acad. Sci. USA* **2001**, *98*, 5116–5121. [CrossRef]
- Wirth, H.; Löffler, M.; Von Bergen, M.; Binder, H. Expression cartography of human tissues using self organizing maps. *BMC Bioinform.* **2011**, *12*, 306. [CrossRef]

21. Yang, X.; Lu, M.; Wang, Y.; Wang, Y.; Liu, Z.; Chen, S. Response Mechanism of Plants to Drought Stress. *Horticulturae* **2021**, *7*, 50. [[CrossRef](#)]
22. Urao, T.; Yamaguchi-Shinozaki, K.; Urao, S.; Shinozaki, K. An Arabidopsis myb homolog is induced by dehydration stress and its gene product binds to the conserved MYB recognition sequence. *Plant Cell* **1993**, *5*, 1529–1539. [[CrossRef](#)] [[PubMed](#)]
23. Chen, B.-J.; Wang, Y.; Hu, Y.-L.; Wu, Q.; Lin, Z.-P. Cloning and characterization of a drought-inducible MYB gene from *Boea crassifolia*. *Plant Sci.* **2005**, *168*, 493–500. [[CrossRef](#)]
24. Jung, C.; Seo, J.S.; Han, S.W.; Koo, Y.J.; Kim, C.H.; Song, S.I.; Nahm, B.H.; Choi, Y.D.; Cheong, J.-J. Overexpression of AtMYB44 Enhances Stomatal Closure to Confer Abiotic Stress Tolerance in Transgenic Arabidopsis. *Plant Physiol.* **2008**, *146*, 323–324. [[CrossRef](#)]
25. SSeo, P.J.; Xiang, F.; Qiao, M.; Park, J.-Y.; Na Lee, Y.; Kim, S.-G.; Lee, Y.-H.; Park, W.J.; Park, C.-M. The MYB96 Transcription Factor Mediates Abscisic Acid Signaling during Drought Stress Response in Arabidopsis. *Plant Physiol.* **2009**, *151*, 275–289. [[CrossRef](#)]
26. Prabu, G.; Prasad, D.T. Functional characterization of sugarcane MYB transcription factor gene promoter (PScMYBAS1) in response to abiotic stresses and hormones. *Plant Cell Rep.* **2012**, *31*, 661–669. [[CrossRef](#)]
27. Wang, X.; Niu, Y.; Zheng, Y. Multiple Functions of MYB Transcription Factors in Abiotic Stress Responses. *Int. J. Mol. Sci.* **2021**, *22*, 6125. [[CrossRef](#)]
28. Li, S.; Khoso, M.A.; Wu, J.; Yu, B.; Wagan, S.; Liu, L. Exploring the mechanisms of WRKY transcription factors and regulated pathways in response to abiotic stress. *Plant Stress* **2024**, *12*, 100429. [[CrossRef](#)]
29. Ando, S.; Nomoto, M.; Iwakawa, H.; Vial-Pradel, S.; Luo, L.; Sasabe, M.; Ohbayashi, I.; Yamamoto, K.T.; Tada, Y.; Sugiyama, M.; et al. Arabidopsis ASYMMETRIC LEAVES2 and Nucleolar Factors Are Coordinately Involved in the Perinucleolar Patterning of AS2 Bodies and Leaf Development. *Plants* **2023**, *12*, 3621. [[CrossRef](#)]
30. Hyndman, D.; Bauman, D.R.; Heredia, V.V.; Penning, T.M. The aldo-keto reductase superfamily homepage. *Chem.-Biol. Interact.* **2003**, *143–144*, 621–631. [[CrossRef](#)]
31. Kirankumar, T.V.; Madhusudhan, K.V.; Nareshkumar, A.; Kiranmai, K.; Lokesh, U.; Venkatesh, B.; Sudhakar, C. Expression Analysis of Aldo-Keto Reductase 1 (AKR1) in Foxtail Millet (*Setaria italica* L.) Subjected to Abiotic Stresses. *Am. J. Plant Sci.* **2016**, *7*, 500–509. [[CrossRef](#)]
32. Boncan, D.A.T.; Tsang, S.S.; Li, C.; Lee, I.H.; Lam, H.-M.; Chan, T.-F.; Hui, J.H. Terpenes and Terpenoids in Plants: Interactions with Environment and Insects. *Int. J. Mol. Sci.* **2020**, *21*, 7382. [[CrossRef](#)] [[PubMed](#)]
33. Tu, M.; Wang, X.; Yin, W.; Wang, Y.; Li, Y.; Zhang, G.; Li, Z.; Song, J.; Wang, X. Grapevine VlbZIP30 improves drought resistance by directly activating VvNAC17 and promoting lignin biosynthesis through the regulation of three peroxidase genes. *Hortic. Res.* **2020**, *7*, 150. [[CrossRef](#)] [[PubMed](#)]
34. Han, X.; Zhao, Y.; Chen, Y.; Xu, J.; Jiang, C.; Wang, X.; Zhuo, R.; Lu, M.-Z.; Zhang, J. Lignin biosynthesis and accumulation in response to abiotic stresses in woody plants. *For. Res.* **2022**, *2*, 9. [[CrossRef](#)]
35. Malerba, M.; Cerana, R. Chitin- and Chitosan-Based Derivatives in Plant Protection against Biotic and Abiotic Stresses and in Recovery of Contaminated Soil and Water. *Polysaccharides* **2020**, *1*, 21–30. [[CrossRef](#)]
36. Pratyusha, D.S.; Sarada, D.V.L. MYB transcription factors—Master regulators of phenylpropanoid biosynthesis and diverse developmental and stress responses. *Plant Cell Rep.* **2022**, *41*, 2245–2260. [[CrossRef](#)] [[PubMed](#)]
37. Czermel, S.; Stracke, R.; Weisshaar, B.; Cordon, N.; Harris, N.N.; Walker, A.R.; Robinson, S.P.; Bogs, J. The Grapevine R2R3-MYB Transcription Factor VvMYBF1 Regulates Flavonol Synthesis in Developing Grape Berries. *Plant Physiol.* **2009**, *151*, 1513–1530. [[CrossRef](#)]
38. Machida, Y.; Suzuki, T.; Sasabe, M.; Iwakawa, H.; Kojima, S.; Machida, C. Arabidopsis ASYMMETRIC LEAVES2 (AS2): Roles in plant morphogenesis, cell division, and pathogenesis. *J. Plant Res.* **2022**, *135*, 3–14. [[CrossRef](#)]
39. Goyal, P.; Devi, R.; Verma, B.; Hussain, S.; Arora, P.; Tabassum, R.; Gupta, S. WRKY transcription factors: Evolution, regulation, and functional diversity in plants. *Protoplasma* **2023**, *260*, 331–348. [[CrossRef](#)]
40. Huang, H.; Ullah, F.; Zhou, D.-X.; Yi, M.; Zhao, Y. Mechanisms of ROS Regulation of Plant Development and Stress Responses. *Front. Plant Sci.* **2019**, *10*, 800. [[CrossRef](#)]
41. Kumari, S.; Nazir, F.; Maheshwari, C.; Kaur, H.; Gupta, R.; Siddique, K.H.; Khan, M.I.R. Plant hormones and secondary metabolites under environmental stresses: Enlightening defense molecules. *Plant Physiol. Biochem.* **2024**, *206*, 108238. [[CrossRef](#)] [[PubMed](#)]
42. Muhammad, D.; Alameedin, H.F.; Oh, S.; Montgomery, B.L.; Warpeha, K.M. Arogenate dehydratases: Unique roles in light-directed development during the seed-to-seedling transition in *Arabidopsis thaliana*. *Front. Plant Sci.* **2023**, *14*, 1220732. [[CrossRef](#)] [[PubMed](#)]
43. Singh, M.; Kumar, J.; Singh, S.; Singh, V.P.; Prasad, S.M. Roles of osmoprotectants in improving salinity and drought tolerance in plants: A review. *Rev. Environ. Sci. Bio. Technol.* **2015**, *14*, 407–426. [[CrossRef](#)]
44. Xu, Z.; Zhang, D.; Hu, J.; Zhou, X.; Ye, X.; Reichel, K.L.; Stewart, N.R.; Syrenne, R.D.; Yang, X.; Gao, P.; et al. Comparative genome analysis of lignin biosynthesis gene families across the plant kingdom. *BMC Bioinform.* **2009**, *10*, S3. [[CrossRef](#)]
45. Lu, Y.; Shao, D.; Shi, J.; Huang, Q.; Yang, H.; Jin, M. Strategies for enhancing resveratrol production and the expression of pathway enzymes. *Appl. Microbiol. Biotechnol.* **2016**, *100*, 7407–7421. [[CrossRef](#)]
46. Dubrovina, A.S.; Kiselev, K.V. Regulation of stilbene biosynthesis in plants. *Planta* **2017**, *246*, 597–623. [[CrossRef](#)]

47. Roy, S.; Mishra, M.; Dhankher, O.P.; Singla-Pareek, S.L.; Pareek, A. Molecular Chaperones: Key Players of Abiotic Stress Response in Plants. In *Genetic Enhancement of Crops for Tolerance to Abiotic Stress: Mechanisms and Approaches, Vol I*; Rajpal, V.R., Sehgal, D., Kumar, A., Raina, S.N., Eds.; Springer: Berlin/Heidelberg, Germany, 2019; pp. 125–165. [CrossRef]
48. Khatri, P.; Chen, L.; Rajcan, I.; Dhaubhadel, S. Functional characterization of Cinnamate 4-hydroxylase gene family in soybean (*Glycine max*). *PLoS ONE* **2023**, *18*, e0285698. [CrossRef]
49. Kriegshauser, L.; Knosp, S.; Grienberger, E.; Tatsumi, K.; Gütle, D.D.; Sørensen, I.; Herrgott, L.; Zumsteg, J.; Rose, J.K.C.; Reski, R.; et al. Function of the HYDROXYCINNAMOYL-CoA:SHIKIMATE HYDROXYCINNAMOYL TRANSFERASE is evolutionarily conserved in embryophytes. *Plant Cell* **2021**, *33*, 1472–1491. [CrossRef]
50. Serrani-Yarce, J.C.; Escamilla-Trevino, L.; Barros, J.; Gallego-Giraldo, L.; Pu, Y.; Ragauskas, A.; Dixon, R.A. Targeting hydroxycinnamoyl CoA: Shikimate hydroxycinnamoyl transferase for lignin modification in *Brachypodium distachyon*. *Biotechnol. Biofuels* **2021**, *14*, 50. [CrossRef]
51. Petersen, M. Hydroxycinnamoyltransferases in plant metabolism. *Phytochem. Rev.* **2016**, *15*, 699–727. [CrossRef]
52. Giordano, D.; Provenzano, S.; Ferrandino, A.; Vitali, M.; Pagliarani, C.; Roman, F.; Cardinale, F.; Castellarin, S.D.; Schubert, A. Characterization of a multifunctional caffeoyl-CoA O-methyltransferase activated in grape berries upon drought stress. *Plant Physiol. Biochem.* **2016**, *101*, 23–32. [CrossRef]
53. Austin, M.B.; Bowman, M.E.; Ferrer, J.-L.; Schröder, J.; Noel, J.P. An Aldol Switch Discovered in Stilbene Synthases Mediates Cyclization Specificity of Type III Polyketide Synthases. *Chem. Biol.* **2004**, *11*, 1179–1194. [CrossRef] [PubMed]
54. Schmidlin, L.; Poutaraud, A.; Claudel, P.; Mestre, P.; Prado, E.; Santos-Rosa, M.; Wiedemann-Merdinoglu, S.; Karst, F.; Merdinoglu, D.; Hugueney, P. A Stress-Inducible Resveratrol O-Methyltransferase Involved in the Biosynthesis of Pterostilbene in Grapevine. *Plant Physiol.* **2008**, *148*, 1630–1639. [CrossRef]
55. Tunc-Ozdemir, M.; Miller, G.; Song, L.; Kim, J.; Sodek, A.; Koussevitzky, S.; Misra, A.N.; Mittler, R.; Shintani, D. Thiamin confers enhanced tolerance to oxidative stress in *Arabidopsis*. *Plant Physiol.* **2009**, *151*, 421–432. [CrossRef] [PubMed]
56. Tian, S.; Wang, D.; Yang, L.; Zhang, Z.; Liu, Y. A systematic review of 1-Deoxy-D-xylulose-5-phosphate synthase in terpenoid biosynthesis in plants. *Plant Growth Regul.* **2022**, *96*, 221–235. [CrossRef]
57. Battilana, J.; Costantini, L.; Emanuelli, F.; Sevini, F.; Segala, C.; Moser, S.; Velasco, R.; Versini, G.; Grando, M.S. The 1-deoxy-d-xylulose 5-phosphate synthase gene co-localizes with a major QTL affecting monoterpene content in grapevine. *Theor. Appl. Genet.* **2009**, *118*, 653–669. [CrossRef]
58. Lange, B.M.; Ghassemian, M. Genome organization in *Arabidopsis thaliana*: A survey for genes involved in isoprenoid and chlorophyll metabolism. *Plant Mol. Biol.* **2003**, *51*, 925–948. [CrossRef]
59. Zhang, S.; Ding, G.; He, W.; Liu, K.; Luo, Y.; Tang, J.; He, N. Functional Characterization of the 1-Deoxy-D-Xylulose 5-Phosphate Synthase Genes in *Morus nobilis*. *Front. Plant Sci.* **2020**, *11*, 1142. [CrossRef]
60. Kambampati, R.; Lauhon, C.T. Evidence for the Transfer of Sulfane Sulfur from IscS to ThiI during the in vitro Biosynthesis of 4-Thiouridine in *Escherichia coli* tRNA. *J. Biol. Chem.* **2000**, *275*, 10727–10730. [CrossRef]
61. Larsson, O.; Wahlestedt, C.; Timmons, J.A. Considerations when using the significance analysis of microarrays (SAM) algorithm. *BMC Bioinform.* **2005**, *6*, 129. [CrossRef]
62. Löffler-Wirth, H.; Kalcher, M.; Binder, H. oposSOM: R-package for high-dimensional portraying of genome-wide expression landscapes on bioconductor. *Bioinformatics* **2015**, *31*, 3225–3227. [CrossRef]
63. Kohonen, T. Self-organized formation of topologically correct feature maps. *Biol. Cybern.* **1982**, *43*, 59–69. [CrossRef]
64. Wirth, H.; Bergen, M.; von Binder, H. Mining SOM expression portraits: Feature selection and integrating concepts of molecular function. *BioData Min.* **2012**, *5*, 18. [CrossRef] [PubMed]
65. Hopp, L.; Wirth, H.; Fasold, M.; Binder, H. Portraying the expression landscapes of cancer subtypes: A case study of glioblastoma multiforme and prostate cancer. *Syst. Biomed.* **2013**, *1*, 99–121. [CrossRef]
66. Loeffler-Wirth, H.; Kreuz, M.; Hopp, L.; Arakelyan, A.; Haake, A.; Cogliatti, S.B.; Feller, A.C.; Hansmann, M.-L.; Lenze, D.; Möller, P.; et al. A modular transcriptome map of mature B cell lymphomas. *Genome Med.* **2019**, *11*, 27. [CrossRef] [PubMed]
67. Prieto, J.A.; Lebon, É.; Ojeda, H. Stomatal behavior of different grapevine cultivars in response to soil water status and air water vapor pressure deficit. *OENO One* **2010**, *44*, 9. [CrossRef]
68. Coupel-Ledru, A.; Lebon, É.; Christophe, A.; Doligez, A.; Cabrera-Bosquet, L.; Péchier, P.; Hamard, P.; This, P.; Simonneau, T. Genetic variation in a grapevine progeny (*Vitis vinifera* L. cvs Grenache × Syrah) reveals inconsistencies between maintenance of daytime leaf water potential and response of transpiration rate under drought. *J. Exp. Bot.* **2014**, *65*, 6205–6218. [CrossRef]
69. Coupel-Ledru, A.; Tyerman, S.D.; Masclef, D.; Lebon, E.; Christophe, A.; Edwards, E.J.; Simonneau, T. Abscisic Acid Down-Regulates Hydraulic Conductance of Grapevine Leaves in Isohydric Genotypes Only. *Plant Physiol.* **2017**, *175*, 1121–1134. [CrossRef]
70. Zhang, W.; Wang, S.-C.; Li, Y. Molecular mechanism of thiamine in mitigating drought stress in Chinese wingnut (*Pterocarya stenoptera*): Insights from transcriptomics. *Ecotoxicol. Environ. Saf.* **2023**, *263*, 115307. [CrossRef]
71. Rapala-Kozik, M.; Wolak, N.; Kujda, M.; Banas, A.K. The upregulation of thiamine (vitamin B1) biosynthesis in *Arabidopsis thaliana* seedlings under salt and osmotic stress conditions is mediated by abscisic acid at the early stages of this stress response. *BMC Plant Biol.* **2012**, *12*, 2. [CrossRef]
72. Ye, X.-F.; Li, Y.; Liu, H.-L.; He, Y.-X. Physiological analysis and transcriptome sequencing reveal the effects of drier air humidity stress on *Pterocarya stenoptera*. *Genomics* **2020**, *112*, 5005–5011. [CrossRef]

73. Li, Y.; Si, Y.-T.; He, Y.-X.; Li, J.-X. Comparative analysis of drought-responsive and -adaptive genes in Chinese wingnut (*Pterocarya stenoptera* C. DC). *BMC Genomics* **2021**, *22*, 155. [[CrossRef](#)]
74. Kinsella, R.J.; Kähäri, A.; Haider, S.; Zamora, J.; Proctor, G.; Spudich, G.; Almeida-King, J.; Staines, D.; Derwent, P.; Kerhornou, A.; et al. Ensembl BioMarts: A hub for data retrieval across taxonomic space. *Database* **2011**, *2011*, bar030. [[CrossRef](#)] [[PubMed](#)]
75. Yates, A.D.; Allen, J.; Amode, R.M.; Azov, A.G.; Barba, M.; Becerra, A.; Bhai, J.; I Campbell, L.; Martinez, M.C.; Chakiachvili, M.; et al. Ensembl Genomes 2022: An expanding genome resource for non-vertebrates. *Nucleic Acids Res.* **2022**, *50*, D996–D1003. [[CrossRef](#)]
76. Kanehisa, M. KEGG: Kyoto Encyclopedia of Genes and Genomes. *Nucleic Acids Res.* **2000**, *28*, 27–30. [[CrossRef](#)] [[PubMed](#)]
77. Grimpel, J.; Cramer, G.R.; Dickerson, J.A.; Mathiason, K.; Hemert, J.V.; Fennell, A.Y. VitisNet: “Omics” Integration through Grapevine Molecular Networks. *PLoS ONE* **2009**, *4*, e8365. [[CrossRef](#)] [[PubMed](#)]
78. Thomas, P.D.; Ebert, D.; Muruganujan, A.; Mushayahama, T.; Albou, L.-P.; Mi, H. PANTHER: Making genome-scale phylogenetics accessible to all. *Protein Sci.* **2022**, *31*, 8–22. [[CrossRef](#)]

Disclaimer/Publisher’s Note: The statements, opinions and data contained in all publications are solely those of the individual author(s) and contributor(s) and not of MDPI and/or the editor(s). MDPI and/or the editor(s) disclaim responsibility for any injury to people or property resulting from any ideas, methods, instructions or products referred to in the content.